

Ehsanul Hoque Apu

MIGRATION AND INVASION
PATTERN ANALYSIS OF ORAL
CANCER CELLS *IN VITRO*

UNIVERSITY OF OULU GRADUATE SCHOOL;
UNIVERSITY OF OULU,
FACULTY OF MEDICINE;
MEDICAL RESEARCH CENTER OULU



ACTA UNIVERSITATIS OULUENSIS
D Medica 1479

EHSANUL HOQUE APU

**MIGRATION AND INVASION
PATTERN ANALYSIS OF ORAL
CANCER CELLS *IN VITRO***

Academic dissertation to be presented with the assent
of the Doctoral Training Committee of Health and
Biosciences of the University of Oulu for public defence
in Auditorium H1091 in Dentopolis, on 19 October
2018, at 12 noon

UNIVERSITY OF OULU, OULU 2018

Copyright © 2018
Acta Univ. Oul. D 1479, 2018

Supervised by
Professor Tuula Salo

Reviewed by
Professor Elizabeth Ferreira Martinez
Doctor Matthew Caley

Opponent
Professor Matthias Nees

ISBN 978-952-62-2022-2 (Paperback)
ISBN 978-952-62-2023-9 (PDF)

ISSN 0355-3221 (Printed)
ISSN 1796-2234 (Online)

Cover Design
Raimo Ahonen

JUVENES PRINT
TAMPERE 2018

Hoque Apu, Ehsanul, Migration and invasion pattern analysis of oral cancer cells *in vitro*.

University of Oulu Graduate School; University of Oulu, Faculty of Medicine; Medical Research Center Oulu

Acta Univ. Oul. D 1479, 2018

University of Oulu, P.O. Box 8000, FI-90014 University of Oulu, Finland

Abstract

Desmoglein 3 (Dsg3) is an adhesion receptor in desmosomes, but relatively little is known about its role in cancer. In this study, the function of Dsg3 was investigated in oral squamous cell carcinoma (SCC) cell lines *in vitro* using locally established human leiomyoma tumor microenvironment (TME) matrices. Since Dsg3 has been identified as a key regulator in cell adhesion, we hypothesized that it may play a role in oral SCC cells adhesion and motility. Thus, one aim of the study was to explore this hypothesis by both gain and loss of function methods in four human buccal mucosa SCC SqCC/Y1 cell lines: transduction of vector control (Ct), full-length (FL) or two different C-terminally truncated Dsg3 mutants (Δ 238 and Δ 560). Live cell imaging was performed for 2D migration and 3D sandwich, alongside other assays. In 3D sandwich, we tested the effects of the monoclonal antibody, AK23, targeting the extracellular domain of Dsg3 in SqCC/Y1 cells. Our results showed that loss of Dsg3 disrupted cell adhesion and protein expression. In 2D assays, FL and Dsg3 mutants migrated faster with higher accumulated distances than Ct. In contrast with 2D, mutants showed accelerated invasion over the Ct in 3D models. The AK23 antibody inhibited only the invasion of FL cells.

The TME *in vivo* consists of cellular and matrix elements playing a leading role in carcinoma progression. To study carcinoma cells invasion *in vitro*, mouse Matrigel® and rat type I collagen are the most commonly used matrices in 3D models. Since they are non-human in origin, they do not perfectly mimic human TME. To address this, we have developed a solid organotypic myoma disc model derived from human uterus leiomyoma tumor. Here, we introduce a novel Myogel, prepared from leiomyoma similar to Matrigel®. We validated Myogel for cell-TME interactions in 3D models, using SqCC/Y1 and HSC-3 cell lines. Compared with Matrigel® and type I collagen, oral SCC cell lines invaded more efficiently in Myogel containing matrices.

This study describes promising 3D models using human TME mimicking Myogel which is suitable to analyze oral SCC cells both in carcinoma monocultures and in co-cultures, such as with TME fibroblasts. We also introduce a possible novel therapeutic target against Dsg3 to suppress cancer cell invasion.

Keywords: carcinoma invasion, cell migration, cell tracking, co-culture, confocal microscopy, desmoglein 3, desmosomes, fibroblasts, live cell imaging, monoclonal antibody, Myogel, myoma discs, oral squamous cell carcinoma, three-dimensional cell culture, tumor microenvironment

Hoque Apu, Ehsanul, Suusyöpäsolujen migraatio- ja invaasiomallien analyysi *in vitro*.

Oulun yliopiston tutkijakoulu; Oulun yliopisto, Lääketieteellinen tiedekunta; Medical Research Center Oulu

Acta Univ. Oul. D 1479, 2018

Oulun yliopisto, PL 8000, 90014 Oulun yliopisto

Tiivistelmä

Desmogleiini 3 (Dsg3) on desmosomien adheesioreseptori, jonka merkityksestä syövässä tiedetään vähän. Koska Dsg3 on tärkeä epiteelisolujen välisissä liitoksissa, oletimme sillä olevan vaikutusta myös suun karsinoomasolujen tarttumisessa ja niiden liikkuvuudessa. Testasimme hypoteesiamme muuttamalla Dsg3:n toimintaa ihmisen posken karsinoomasolulinjassa SqCC/Y1, josta oli aiemmin valmistettu neljä erilaista muunnosta: tyhjän vektorin sisältävä kontrollisolulinja (Ct), kokopitkää Dsg3 tuottava solulinja (FL), sekä kaksi Dsg3 C-päästä lyhennettyä mutanttisolulinjaa ($\Delta 238$ ja $\Delta 560$). Immunofluoresenssi-menetelmää käyttäen analysoimme solulinjoissamme solujen välisiä liitoksia. Lisäksi mittasimme solujen liikkeitä 2D-migraatio- ja 3D-sandwich-kokeissa. Testasimme myös Dsg3:n solunulkoista osaa tunnistavan monoklonaalisen vasta-aineen (AK23) vaikutusta solujen invaasioon. Osoitimme, että Dsg3:n rakenteen muuttaminen ja toiminnan estyminen häiritsi solujen tarttumista. 2D-kokeissa sekä FL että mutanttilinjat ($\Delta 238$ ja $\Delta 560$) migroivat kontrollisoluja nopeammin ja pidemmälle, mutta 3D-kokeissa vain mutanttilinjat invasoituivat kontrollisoluja tehokkaammin. AK23-vasta-aine esti vain FL-solujen invaasiota.

Syöpäsolujen 3D-invaasiota mittaavissa kokeissa käytetään yleensä hiiren kasvaimesta valmistettua kaupallista Matrigeeliä® tai rotan kudoksista eristettyä tyyppin I kollageenia. Tutkimusryhmämme on jo aiemmin kehittänyt organotyyppisen myoomamallin, jossa valmistamme myoomakudosnapit ihmisen kohdun leiomyoomakasvaimista. Tässä työssä valmistimme leiomyoomasta Myogeelia, vertasimme sitä Matrigeeliin®, sekä tutkimme tarkemmin Myogeeli-vaikuteen soveltuvuutta 3D-tutkimuksiin. Totesimme, että kielen (HSC-3) ja posken (SqCC/Y1) karsinoomasolut invasoituivat tehokkaimmin Myogeeli-pitoisissa matrikeissa kuin Matrigeeliä® tai kollageeniä sisältävissä kasvatusalustoissa. Tutkimustulostemme perusteella Myogeeli-pohjaiset 3D-mallit soveltuvat hyvin sekä syöpäsolulinjojen invaasiotutkimuksiin että yhteisviljelmiin, joissa syöpäsoluja viljellään yhdessä syöpäkasvaimen ympärillä olevien solujen, kuten fibroblastien, kanssa.

Asiasanat: desmogleiini 3, desmosomi, elävän solun kuvantaminen, fibroblasti, invaasio, kasvaimen mikroympäristö, kolmiulotteinen soluviljely, konfokaalimikroskopia, levyepiteelikarsinooma, monoklonaalinen vasta-aine, Myogeeli, myooma, solujen migraatio, yhteisviljely

*To our creator, my family and people
who suffer from cancer*

Acknowledgements

This study was conducted at the Cancer and Translational Medicine Research Unit, Faculty of Medicine, the University of Oulu, between the years 2014 and 2018.

First, my sincerest gratitude goes to my doctoral supervisor, Professor Tuula Salo for giving me this opportunity to join her research team and pursue my studies under her supervision. Her active support, training and guidance have given me a lot of confidence, and independence in research. Thank you for encouraging and pushing me towards achieving the goals. I am really inspired by her endless ambition and enthusiasm in work and proud to be a part of one of her dream projects, and hope to hear more of her innovative ideas in the coming future. I am also grateful for her valuable and practical advice to build a successful research career.

I want to thank my follow-up group members, Professor Lauri Eklund, Professor Markus Mäkinen and Adjunct Professor Sakari Kellokumpu for approving the doctoral training plan, and monitoring the quality of this work.

I am deeply grateful to Professor Elizabeth Ferreira Martinez and Dr Matthew Caley for taking their valuable time to carefully evaluate this thesis and for their constructive comments, suggestions and remarks. I thank Deborah Kaska for her prompt language checking for this dissertation and my colleague Krista Juurikka for providing the required Finnish translations and other countless co-operation.

I wish to express my gratitude to the staff of Cancer and Translational Medicine Research Unit, Biocenter Oulu, Department of Computer Science and Engineering, and Fibre and Particle Engineering Department of the University of Oulu for allowing me to perform this work in facilities. I would like to thank all my fellow doctoral colleagues and friends in the Medical campus for their support, and friendship, and for the nice times we spent together. Good luck with research!

I would like to thank Dr Hong Wan and her efficient team in Blizzard Institute of Queen Mary, University of London for supporting and collaborating in this study. Also, I am grateful to our study collaborators from the University of Oulu, Professor Lauri Eklund and Professor Janne Heikkilä for their active support.

American Business magnate, Mr Henry Ford once rightfully said, "*Coming together is a beginning. Keeping together is progress. Working together is success.*" I cannot express my full gratitude towards the Tuula Salo group members in one paragraph, in fact it was a remarkable journey together. I thank each of the current, former, regular and visiting members for their moral support, and inspiration during the darkest hours. Thank you Krista Juurikka, Maija Risteli, Priscila Campioni Rodrigues, Virve Pääkkönen, Ramin Akhi, Meeri Sutinen, Elias Sundquist, Ilkka

Alahuhta, Otto Väyrynen, Carolina Bitu, Pirjo Åström, Pia Nyberg, Emma Pirilä, Johanna Korvala, Toni Sandvik, Clarissa Demeda, Wagner Gomes, Maurício Dourado and Marlene Vierthaler. I also thank our colleagues from the Helsinki group, Ahmed Al-Samadi, Katja Tuomainen and Alhadi Almangush. The successful completion of this study was only possible with the technical support from our skilled and co-operative laboratory personnel. From the depth of my heart, I thank Maija-Leena Lehtonen, Tanja Kuusisto and Eeva- Maija Kiljander.

I am grateful to my co-authors, Saad Ullah Akram, Jouni Rissanen, Hanan Moftah, Kasuni Dias, Li Liu, Jutamas Uttagomol, Lesley Bergmeier, Stephanie Kermorgant, Nilva Cervigne, Carine Oliveira, Steffen Ohlmeier, Pirjo Juusela, Markku Santala, Kalle Savolainen, Adriana Franco Paes Leme and Ricardo Coletta.

Outside the professional circle, I would like to thank my parents, younger brothers, all my family and my wife's family members for their support and understanding. I am deeply grateful to my respected mother, Nasreen Jahan Mita and father, Dr Mohammad Shamsul Hoque, for their sacrifices to fulfill my dreams. I thank both of you to believe in me and always being there when I needed the most.

Finally, I would like to thank my beloved wife Dr Nazeeba Siddika for her big support, for helping and tolerating me throughout these years. Despite the countless difficult times, you believed in me and were a source of inspiration, and encouragement. Thank you for listening and understanding me at all times. Your performance as a doctoral student also encouraged me a lot and hope to learn Meta-analysis from you. Big cheers to our little daughter Elisha, for co-operating her mother while I was away from home in most weekends to complete the study.

Special thanks and appreciation goes to the Bangladeshi post-graduate students and their family members currently studying in the University of Oulu. Especially, I am grateful to fellow doctoral students and my friends, Shahriar Shahabuddin, Tirthankar Paul, and Dr Atiqul Haq Mazumder for their encouragement, true friendship and moral support during these years. Among other university friends, I thank Sandhanakrishnan Cattavarayane and Al-Tamini Tapu for their support.

This study was financially supported by Sigrid Juselius Foundation, Tyyni Tani Foundation, Finnish Dental Society Apollonia, The University of Oulu Scholarship Foundation, and Centre for International Mobility (CIMO) and research funds from the Medical Faculty of the University of Oulu and Oulu University Hospital special state support for research.

Oulu, August 2018

Ehsanul Hoque Apu

Abbreviations

Δ C	C-terminally truncated desmoglein 3 mutants
2D	two dimensional
3D	three dimensional
A431	human epidermoid carcinoma cell line
Abs	antibodies
AJCC	American Joint Committee on Cancer
AJs	adherens junctions
AK	acantholytic keratinocyte
BM	basement membrane
BSA	bovine serum albumin
Ct	vector control
C-terminal	carboxyl-terminal end
Dsc	desmocollin
Dsg	desmoglein
Dsg3	desmoglein 3
DSMs	desmosomes
FL	overexpressed full length desmoglein 3
PV	pemphigus vulgaris
BD	budding-depth
CAFs	human carcinoma-associated fibroblasts
DMEM	Dulbecco's Modified Eagle Medium
ECD	extracellular domain
ECM	extracellular matrix
EHS	Engelbreth-Holm-Swarm
EGF(R)	epidermal growth factor (receptor)
EMT	epithelial-mesenchymal transition
FBS	fetal bovine serum
FGF-2	fibroblast growth factor 2
FN	fibronectin
GFP	green fluorescent protein
GFs	human gingival fibroblasts
H2B	Histone H2B
HaCaT	human immortal keratinocyte cell line
HGF	hepatocyte growth factor
HPV	human papilloma virus

HSC-3	human tongue squamous cell carcinoma cell line
IgG	immunoglobulin G
ICD	intracellular domains
IMF	immunofluorescence
kDa	kilo Dalton
KGM	Keratinocyte Growth Medium
LMA	low-melting agarose
LOX	lysyl oxidase
MDCK	mammalian Madin-Darby Canine Kidney cell line
MMP	matrix metalloproteinase
NaCl	sodium chloride
NOFs	human normal oral fibroblasts
N-terminal	amino-terminal end
OSCC	oral squamous cell carcinoma
OTSCC	oral (mobile or anterior) tongue squamous cell carcinoma
PBS	phosphate-buffered saline
Pg	plakoglobin
RNAi	RNA interference
SCC	squamous cell carcinoma
shRNA	small hairpin RNA
SqCC/Y1	human oral buccal squamous cell carcinoma cell line
TCA	trichloroacetic acid
TGF- β	transforming growth factor beta
TME	tumor microenvironment
TMEM	tumor microenvironment matrix
TNC	tenascin-C
TNM	tumor, node, and metastasis

Original publications

- I Moftah H, Dias K, Hoque Apu E, Liu L, Uttagamol J, Bergmeier L, Kermorgant S & Wan H. (2017). Desmoglein 3 regulates membrane trafficking of cadherins, an implication in cell-cell adhesion. *Cell Adh Migr*, 11 (3), 211-232.
- II Salo T, Sutinen M, Hoque Apu E, Sundquist E, Cervigne N, Oliveira CE, Akram SU, Ohlmeier S, Suomi F, Eklund L, Juusela P, Åström P, Bitu CC, Santala M, Savolainen K, Korvala J, Paes Leme AF & Coletta RD. (2015). A novel human leiomyoma tissue derived matrix for cell culture studies. *BMC Cancer*, 15:981.
- III Hoque Apu E, Akram SU, Rissanen J, Wan H & Salo T. (2018). Desmoglein 3 – influence on oral carcinoma cell migration and invasion. *Exp Cell Res*, 370 (2), 376-389.

Reprinted with permission from Taylor & Francis (I), Springer Nature (II) and Elsevier Limited (III).

Original publications are not included in the electronic version of the dissertation.

Contents

Abstract	
Tiivistelmä	
Acknowledgements	9
Abbreviations	11
Original publications	13
Contents	15
1 Introduction	17
2 Review of the literature	19
2.1 Oral squamous cell carcinoma (OSCC)	19
2.1.1 Risk factors for OSCC.....	19
2.1.2 Diagnosis and treatment of OSCC.....	20
2.2 Oral mucosa and cell junctions	23
2.2.1 Desmosomes (DSMs).....	25
2.2.2 Structure of DSMs.....	25
2.2.3 Composition of DSMs.....	26
2.2.4 Functions of DSMs.....	27
2.3 Desmoglein 3 (Dsg3)	29
2.3.1 Dsg3 structure.....	29
2.3.2 Dsg3 signaling.....	30
2.3.3 Dsg3 in disease.....	30
2.3.4 Dsg3 as an anti-cancer drug target	31
2.3.5 Expression of Dsg3 C-terminally truncated proteins and their dominant negative effect on cell-cell adhesions.....	32
2.4 Tumor microenvironment (TME)	34
2.4.1 Composition of TME.....	34
2.4.2 Role of TME in cancer progression.....	34
2.4.3 TME matrices	36
2.4.4 Three dimensional (3D) TME matrix models	38
3 Aims of the present study	43
4 Materials and methods	45
4.1 Cell cultures (I, II, III).....	47
4.1.1 Carcinoma cell lines and their characteristics (I, II, III).....	47
4.1.2 Other cell lines (III).....	47
4.2 Lentiviral transduction (II, III).....	48
4.3 Dispase dissociation assay (I)	48

4.4	Immunofluorescence (I, III)	49
4.5	Horizontal migration (III)	49
4.6	Myoma discs and Myogel (II, III)	50
4.6.1	Rheology of Myogel (III)	51
4.7	Vertical migration and invasion assay (III)	51
4.8	Hanging drop spheroid cultures (II)	52
4.9	Adhesion assay (II, III)	52
4.10	Immunofluorescence (IMF) in coated coverslips (III)	53
4.11	3D hanging drop method (II)	53
4.12	3D sandwich culture (III)	54
4.13	AK23 antibody treatment against Dsg3 (III)	54
4.14	3D image acquisition and time-lapse microscopy	55
4.14.1	Spinning disc confocal microscopy (II)	55
4.14.2	Epifluorescence microscopy and deconvolution (III)	55
4.15	Myoma disc assay (III)	55
4.16	Statistical analysis (I, II, III)	56
4.17	Ethical considerations (II, III)	56
5	Results	57
5.1	Detecting C-terminally truncated mutants	57
5.2	Expression of Dsg3 truncated proteins caused compromised cell-cell adhesions	58
5.3	Dsg3 affects both horizontal and vertical migration in buccal carcinoma cells	59
5.4	Myogel is a novel matrix for studying carcinoma cell invasion	59
5.5	Buccal SCC cells invade faster in leiomyoma derived matrices	60
5.6	OSCC cell invasion depends on the microenvironment	61
5.6.1	Tongue SCC cell invasion in 3D hanging drops	61
5.6.2	Buccal SCC cell invasion in 3D sandwich	61
5.7	OSCC cells interact with fibroblasts in 3D sandwich	62
5.8	Antibody treatment alters the invasion pattern in buccal SCC cells in 3D sandwich	62
6	Discussion	63
6.1	Dsg3 promotes migration and invasion of OSCC cell lines	63
6.2	Leiomyoma derived TME matrices affect OSCC cell invasion	64
6.3	Dsg3 as a potential novel anti-cancer drug target	67
	List of references	69
	Original publications	83

1 Introduction

Desmosomes (DSMs) are specialized intercellular junctions from the cadherin superfamily (Schmidt & Koch, 2007). Desmoglein 3 (Dsg3) is a member of the desmoglein subfamily serving as an adhesion receptor in DSMs, and it is best known as a pemphigus vulgaris (PV) antigen. Although a panel of studies have indicated that Dsg3 plays a pivotal role in cell cohesion, relatively little is known about its actual role in cancer (Brown & Wan, 2015). A correlation study between Dsg3 expression level and cancer progression suggested that Dsg3 might contribute to cancer spreading (Brown & Wan, 2015). In support of the suggestion that Dsg3 has a role in cancer, our previous report revealed that overexpression of Dsg3 enhances cell migration and invasion of epidermoid carcinoma, and oral buccal mucosa squamous cell carcinoma (SCC) SqCC/Y1 cell lines *in vitro* (Brown et al., 2014; Tsang et al., 2010). Dsg3 has an oncogenic role over growth, as well as in the invasion of oral squamous cell carcinoma (OSCC) cells through the Dsg3-plakoglobin-TCF/LEF pathway (Chen et al., 2013). Moreover, RNAi and shRNA knockdown of Dsg3 inhibits growth, migration, and invasion of OSCC cell lines, suggesting Dsg3 functions in more than just cell-cell adhesion (Chen et al., 2007; Chen et al., 2013).

The tumor microenvironment (TME) plays a leading role in invasion and metastasis. It consists of blood vessels, carcinoma-associated fibroblasts (CAFs), inflammatory cells, ECM molecules and their gradients (Salo et al., 2014). Conventional cancer cell studies have focused primarily on two dimensional (2D) *in vitro* models. Although the 2D analyses help to illuminate mechanical details of cell-substrate or cell-cell interactions, they do not accurately mimic *in vivo* cell-matrix interactions. Genetically engineered rat, mouse and zebrafish are commonly used *in vivo* models in cancer research. In cancer drug development for personalized and targeted therapies, patient-derived tumor xenograft in animal models are widely used *in vivo* (Yee, Ignatenko, Finnberg, Lee, & Stairs, 2015). *In vitro* three dimensional (3D) culture models utilizing human TME matrices cover the gap between 2D culture and *in vivo* models (Salo et al., 2018).

2 Review of the literature

2.1 Oral squamous cell carcinoma (OSCC)

Oral cancer is a deadly disease and according to GLOBACAN 2012, lip and oral cavity cancer is the world's eighth most frequent cancer in men living in less developed countries. Worldwide in 2012, there were around 300,000 new cases of the lip and oral cavity cancers, an estimated 145,000 deaths from these diseases. In Asia, 168,850 new lip and oral cavity cancers were diagnosed (Ferlay et al., 2013; Ferlay et al., 2015). Almost 90% of the cancer cases in the head and neck region are diagnosed as oral squamous cell carcinoma (OSCC), which differ from other carcinomas in terms of pathogenesis and clinical prognosis (Sathiyasekar, Chandrasekar, Pakash, Kumar, & Jaishlal, 2016). Incidences of OSCC fluctuate significantly between countries, with the highest rates found in South Asia; mostly in India, Pakistan and Bangladesh (Shield et al., 2017). The tongue is among the most frequent sites for intraoral carcinoma, 30% of SCC of the oral cavity in India are diagnosed in the tongue (Sultana, Bashir, & Molla, 2014). Buccal mucosa SCC cancer is often characterized by pain and ulceration, and it appears primarily along the occlusal plane. It has an aggressive nature and growth with a high recurrence rate (Kim & Myoung, 2017).

2.1.1 Risk factors for OSCC

Cigarette-smoking and alcohol consumption are the main risk factors for OSCC in the Western population, whereas smokeless tobacco and areca nut usage are the most common causes of OSCC in Southeast Asia (Joshi, Dutta, Chaturvedi, & Nair, 2014). The combined exposure to cigarettes and/or alcohol lead to an increase of cancer risk (up to 35-fold), among populations consuming at least ten cigarettes/day and 84 g/day of alcohol (Dal Maso et al., 2016). In the Asia-Pacific area, Betel quid chewing is the most common form of tobacco consumption, which includes areca nut, betel leaf and slaked lime (Warnakulasuriya, Trivedy, & Peters, 2002). One-tenth of the world's total population chew betel quid frequently (Gupta & Ray, 2004). The increased amount of tobacco intake has increased the risk of OSCC in developing countries.

In the developed countries, the incidence of oral cavity cancer is decreasing, except in the mobile tongue, whereas it remains unchanged in the developing

countries. A study showed that the five-year survival rate was highest in cases where the tumor was localized in the lip region (Listl et al., 2013). In a study of a European population, tobacco smoking was associated with about 77% of oral cancer cases, whereas alcohol consumption was associated with 52% of the cases (Rodriguez et al., 2004). Areca nut usage is involved with a premalignant condition called oral submucous fibrosis (OSMF), as well as oral cavity cancers (Joshi, Dutta, Chaturvedi, & Nair, 2014). There are also alternative risk factors, such as hepatitis C (Porter, Lodi, Chandler, & Kumar, 1997) and human papillomavirus (HPV) (Shaikh et al., 2017). However, HPV is mainly associated with the base of tongue, tonsils and larynx cancers. Lower socioeconomic status (Agarwal, Sethi, Sareen, & Dhingra, 2011) and poor oral hygiene (Homann et al., 2001) are other contributing factors. There is no direct evidence that any specific diet increases the risk of oral cancer. However, a high intake of processed meat products may increase OSCC risk (Xu, Yang, Wu, Li, & Bai, 2014). A balanced diet with fresh fruits, fibers, and vegetables is recommended to possibly reduce the risk of oral cancer (Taghavi & Yazdi, 2007).

2.1.2 Diagnosis and treatment of OSCC

In the oral cavity, squamous cell carcinoma (OSCC) originates from mucosal keratinocytes. The clinical characteristics of OSCC are usually, but not always, easy to recognize. The common features are red lesions, mixed red and white lesions, lumps, ulcers, pain, bleeding, loose tooth, unhealed extraction socket, and difficulties in chewing and swallowing. To confirm the diagnosis, a representative biopsy and histopathological examination is mandatory. Early diagnosis of OSCC is important to increase the survival chances of the patient: in the early stage (T1) tumors the survival is high, commonly between 80–90%. However, still in Finland more than half of the patients with oral tongue cancers die of the disease (Mroueh et al., 2017). OSCC prognosis depends mostly on tumor size, depth of invasion, resection completeness and nodal involvement (Bagan, Sarrion, & Jimenez, 2010; Scully & Bagan, 2009). The location of the oral cavity cancer is also important for the prognosis. OSCC located in the tongue, soft palate or in the floor of the mouth show the worst clinical prognosis compared to the other locations, such as buccal mucosa or lips (Jadhav & Gupta, 2013).

Cancer staging is an important factor, which affects the treatment of the patient. The American Joint Committee for Cancer (AJCC) staging system assesses three major factors: the extent of the primary tumor (T), the presence or absence and

extent of regional lymph node metastasis (N), and the presence or absence of distant metastasis (M). These factors are combined when tumors are divided into five stages (0-IV). In general, the higher the stage the worse the prognosis (Lydiatt et al., 2017; Sano & Myers, 2007). The AJCC has recently published the 8th edition of the TNM classification (Table 1). One of the main changes compared to the previous 7th edition is that the latest classification includes the depth of invasion (DOI) in the T-category (Edge & American Joint Committee on Cancer, 2017; Lydiatt et al., 2017).

Histological grading of OSCC also has some prognostic value. AJCC recommended general grades for clinical use, if there is no specific system used are: grade X: grade cannot be assessed, grade 1: well differentiated, grade 2: moderately differentiated, grade 3: poorly differentiated, and grade 4: undifferentiated (Edge & American Joint Committee on Cancer, 2017). There are also other grading systems available to study tumor extent such as Bryne's malignancy system. It is based on five morphologic features, each graded from 1 to 4 (Bryne, Nielsen, Koppang, & Dabelsteen, 1991).

Our research group has developed a novel "BD predictive model" used for oral tongue SCC (OTSCC). In the BD-model, tumor budding (B) and invasion depth (D) are analyzed from the HE-stained resection sections. Tumor budding is defined as the presence (1) or absence (0) of small clusters of less than 5 carcinoma cells at the invasive front using 20 x magnification. The invasion depth is analyzed from the level of the surrounding mucosa basement membrane to the deepest area of the invasion, and the tumors are divided into two categories: cells invading less (value 0), or 4 mm or deeper (value 1). Tumors are BD scored from 0 to 2. The BD score is 0 if both the budding and depth of invasion values are 0; the score is 1 if either the budding or depth of invasion values are 1, and the score is 2, if both budding and depth of invasion values are 1 (Almangush et al., 2014; Almangush et al., 2015).

The main objective of successfully treating OSCC is to restore normal physiology, and function of the affected area after tumor elimination. The ultimate goal is to minimize the treatment duration and prevent any chance of recurrence. Primary treatment outcome depends on various factors considering the tumor, the patient's health, and the physician. Tumor size and its anatomical position are important factors depending on the proximity to the bone, and lymph nodes. The patient's age, general health conditions, previous treatment history, and lifestyle are considered carefully before finalizing any treatment plan. The treatment options include surgery, chemotherapy, radiotherapy, or a combined strategy. Further reconstructive or plastic surgery may also be required in some cases. OSCC and its

treatment may affect the speech, swallowing, and breathing pattern of patients. To overcome these outcomes, speech and physiotherapy options should be considered for rehabilitation (Shah & Gil, 2009).

Table 1. TNM classification of oral cancers (AJCC Cancer Staging Manual, 8th edition)

TNM	Criteria
T	Primary tumor
TX	Primary tumor cannot be assessed
Tis	Carcinoma in situ
T1	Tumor \leq 2 cm, \leq 5 mm depth of invasion (DOI) (DOI is depth of invasion and not tumor thickness)
T2	Tumor \leq 2 cm, DOI $>$ 5 mm and \leq 10 mm or tumor $>$ 2 cm but \leq 4 cm, and \leq 10 mm DOI
T3	Tumor $>$ 4 cm or any tumor $>$ 10 mm DOI
T4	Moderately advanced or very advanced local disease
T4a	Tumor invades through cortical bone or involves the inferior alveolar nerve, floor of mouth, or skin of face (ie, chin or nose); (oral cavity) tumor invades adjacent structures only (eg, through cortical bone of the mandible or maxilla or involves the maxillary sinus or skin of the face)
T4b	tumor invades masticator space, pterygoid plates, or skull base and/or encases the internal carotid artery
N	Regional lymph nodes
NX	Regional lymph nodes cannot be assessed
N0	No regional lymph node metastasis
N1	Metastasis in a single ipsilateral lymph node, \leq 3 cm
N2	Metastasis in a single ipsilateral lymph node, \leq 3 cm or $>$ 3 cm but \leq 6 cm
N2a	Metastasis in a single ipsilateral or contralateral lymph node, \leq 3 cm or in a single ipsilateral lymph node, \leq 3 cm or $>$ 3 cm but \leq 6 cm
N2b	Metastasis in multiple ipsilateral lymph nodes, \leq 6 cm
N2c	Metastasis in bilateral or contralateral lymph nodes, \leq 6 cm
N3	Metastasis in a lymph node $>$ 6 cm, or in a single ipsilateral lymph node $>$ 3 cm; or metastasis in multiple ipsilateral, contralateral, or bilateral lymph nodes
N3a	Metastasis in a lymph node $>$ 6 cm
N3b	Metastasis in a single ipsilateral node $>$ 3 cm; or metastasis in multiple ipsilateral, contralateral, or bilateral lymph nodes
M	Distant metastasis
MX	Distant metastasis cannot be assessed
M0	No distant metastasis
M1	Distant metastasis

2.2 Oral mucosa and cell junctions

General histological features of oral mucosa (OM) present surface epithelium, overlying and adhered to connective tissue at the basement membrane (BM). Deep to the epithelium, the superficial connective tissue or lamina propria covers the deeper submucosa. Surface epithelium of OM is stratified squamous epithelium which can be either keratinized (keratinized) or non-keratinized and provides protection against external stress, and damage (Winning & Townsend, 2000).

Oral epithelium (OE) can be classified into three types according to their morphology and differentiation patterns, such as keratinized stratified squamous epithelium (masticatory mucosa distributed in hard palate and gingiva), non-keratinized stratified squamous epithelium (buccal mucosa, labial mucosa), and specialized mucosa (dorsal surface of the tongue). Both masticatory and specialized mucosae are keratinized in humans (Jones & Klein, 2013; Shetty & Gokul, 2012; Winning & Townsend, 2000). Keratinized OE is identical to the skin epidermis; it is stratified and has basal, spinous, granular, and corneal layers. Non-keratinized OE is also stratified, however, it consists of basal, spinous, intermediate and superficial layers (Jones & Klein, 2013).

Normal cellular attachments are one of the main homeostatic components of the human body. Cell junctions (CJs) formed by different cellular components or cell-to-cell adhesion are essential for the development of multicellular living organizations (Nagafuchi, 2001). Normal cell-cell junctions vary on cell types; however, their primary function is maintaining adhesion and biological integrity, they are essential for the proper cell functioning, and tissue generation (Brooke, Nitoiu, & Kelsell, 2012). Cells interact with their surroundings and underlying extracellular matrix (ECM) through specialized junctional proteins to regulate adhesion, structure and transmit information to the cell interior about the environment (Balda & Matter, 2016). In epithelial cell lines, there are mainly three functional groups of CJs, termed as occluding, communicating, and anchoring junctions (Alberts et al., 2002).

Occluding junctions

Occluding junctions (OJs) are also known as tight junctions. They are a specialized type of junctions and seal cells together in the intercellular space of epithelium and prevents small molecules from leaking from one side to the other (Yokouchi & Kubo, 2018). OJs regulate different signals to guide epithelial proliferation,

polarization and differentiation (Balda & Matter, 2016) and are vital for the barrier function of mammalian skin (Yokouchi & Kubo, 2018).

Communicating junctions

Communicating junctions mediate the transfer of chemical or electrical signals from one interacting cells to partner cells (Alberts et al., 2002). Most epithelial cells communicate through gap junctions (GJs) with their neighbors. GJs link cytoplasm of adjacent cells together through a gap of 2-3 nm in diameter, which acts as a passage of chemical or electrical signals between neighboring cells (Alberts et al., 2002; Mese, Richard, & White, 2007).

Anchoring junctions

The last major group of the functional junctions is the anchoring junctions, they adhere to the cells and their cytoskeletons mechanically to their neighboring components or the ECM. The junctional proteins stretch within the plasma membrane to connect cytoskeletal proteins in one cell to those in neighboring cells or the ECM proteins. AJs are often termed as zonula adherens as their appearance is like continuous zonula. (Mruk, Silvestrini, & Cheng, 2008). They anchor neighboring cells in the form of adhesion belts along the plasma membrane (Niessen and Gottardi, 2008). These junctions transmit stresses and are tethered to cytoskeletal filaments inside the cells. These junctions include both cell-cell adhesions (adherens junctions and desmosomes) and cell-matrix (focal adhesions and hemidesmosomes) adhesions and have the actin filament attachment sites and intermediate filament attachment sites. Among these junctions, adherens junctions (AJs) are the cell-cell junctions that attach to the actin cytoskeleton whereas the desmosomes (DSMs) and hemidesmosomes are the junctions that associate with the intermediate filament network. In normal epithelial tissues, cell-cell junctions are abundant at intercellular spaces, particularly in the suprabasal layers of stratified squamous epithelial tissues. In AJs, they are classical cadherins, E-cadherin and P-cadherin whereas, in DSMs, they comprise desmogleins and desmocollins (Alberts et al., 2002; Mruk, Silvestrini, & Cheng, 2008).

2.2.1 Desmosomes (DSMs)

Desmosomes (DSMs) are anchoring junctions, which provide strong intercellular adhesion in epithelia (Garrod, 2010). DSMs differ from adherens junctions (AJs) because they are tethered to the intermediate filament network, whereas AJs attach to the actin cytoskeleton. DSMs were first identified by Giulio Bizzozero (1846-1901), an Italian pathologist who during his examination of the spinous layer of the epidermis noticed small dense nodules at the contact points between adjacent cells. He identified those structures as cell to cell adhesion points (Culkins & Setzer, 2007; Delva, Tucker, & Kowalczyk, 2009). After this remarkable discovery, further experiments by dedicated research groups provided more detailed information about the composition, structure, and functions of DSMs. Josef Schaffer first described the term 'desmosome' in 1920. Historically, DSMs were considered as static 'spot welds' (Dubash & Green, 2011). Studies using time-lapse fluorescence microscopy revealed that DSMs form exceptionally static, stable and more interconnected cell adhesion (Windoffer, Borchert-Stuhltrager, & Leube, 2002).

Further studies show that DSMs are a significant type of anchoring junction since they anchor stress bearing intermediate filaments at the strong intercellular adhesion sites, and these structures provide mechanical integrity to tissues (Yin & Green, 2004). The DSMs are required to maintain the cohesive properties of tissues, especially in organs which require more stretching and bear more stress. Studies have shown that abnormal signaling and adhesion through these junctions contribute to various epidermal and cardiac disease symptoms (Schmidt & Koch, 2007). These junctions provide hyper adhesion which distinguishes them from other intercellular junctions (Garrod & Chidgey, 2008; Tsang et al., 2012).

2.2.2 Structure of DSMs

By transmission microscopy, DSMs can be divided into three morphologically characterized zones: the extracellular core domain (ECD), the outer dense plaque (ODP) and the inner dense plaque (IDP) (Green & Jones, 1996; North et al., 1999). Their diameter varies between 0.2-0.5 μm , and, for example, in Madin-Darby canine kidney (MDCK) cells DSMs are only approximately 0.22 μm (Al-Amoudi et al., 2004).

DSMs are formed by dense plaques, which are arranged symmetrically on the cytoplasmic faces of the plasma membranes (PM) of adjoining cells, and are approximately 7 nm thick. The ECD is 30 nm wider and has a central dense midline.

Each plaque consists of a 15-20 nm thicker ODP adjacent to the PM, an electron lucent zone (~8 nm), and an IDP (~15-20 nm), which is less dense than the ODP (Thomason, Scothern, McHarg, & Garrod, 2010).

DSMs consist of a protein complex that can be divided into three major families, desmosomal cadherins (desmoglein & desmocollin), plakin (desmoplakin, envoplakin, periplakin, epiplakin, and plectin) and armadillo (plakoglobin, plakophilin, and p120 catenin) (Angst, Marcozzi, & Magee, 2001; Saito, Tucker, Kohlhorst, Niessen, & Kowalczyk, 2012). Desmocollin (Dsc) and desmoglein (Dsg) share 30% amino acid identity with each other and with classical cadherins and have five extracellular cadherin (EC) repeats containing Ca^{2+} binding and cell adhesion recognition (CAR) sites (Thomason, Scothern, McHarg, & Garrod, 2010). The DSMs join the intermediate filaments to form a network called the desmosomes intermediate filament complex (DIFC) in epithelial cells (Garrod & Chidgey, 2008). This complex is essential for strong adhesion and maintenance of epithelial tissue integrity (Brooke, Nitoiu, & Kelsell, 2012).

2.2.3 Composition of DSMs

Desmosomal cadherins

The desmosomal cadherins (DCs) are single-pass transmembrane proteins that are the core protein components in DSMs. They consist of two glycoprotein subfamilies, desmocollin (Dsc) and desmoglein (Dsg), which are required for the formation and function of DSMs (Garrod & Chidgey, 2008). Seven DCs are characterized so far, three Dscs, and four Dsgs (Garrod, Merritt, & Nie, 2002). They help to form a link between two cells by heterophilic or homophilic binding by their extracellular domains to other DCs on an adjacent cell (Mannan et al., 2011). They span the plasma membrane with their C-terminal domains located in the plaque (ODP) and their N-terminal domains connect the two halves of the DSMs together in the intercellular space. All DCs are synthesized with an N-terminal signal and pro-peptides that are cleaved during protein maturation (Garrod & Chidgey, 2008). The genes of Dscs and Dsgs are clustered together in a region of chromosome 18 (Frank et al., 2001).

Armadillo family

The armadillo family members are multifunctional adhesive and signaling proteins. They interact with the DCs, plakins and intermediate filaments. Protein members of this family are Plakoglobin (Pg) and Plakophilins (Pp) (Teh et al., 2011). These proteins are found in the ODP of DSMs; their locations differ in that Pp is located closer to the plasma membrane than Pg (North et al., 1999).

Plakin family

The plakin family members are desmoplakin (DP), envoplakin, periplakin, epiplakin, and plectin. Among them, DPs are the major plaque proteins that bridge between ODP and IDP in DSMs. They mainly link cytokeratin filaments to the DSM junction complexes. DP has two isoforms (DP I and DP II), with molecular weights of 250 kDa and 220 kDa, respectively. DP consists of three domains, the globular C terminus, the N terminus and a central coiled domain through which DP proteins form a parallel dimer (Kitajima, 2002). An essential function of DP in cell-cell adhesion was studied in epidermoid carcinoma cells with depletion of DP. When the endogenous DP was undetectable, the junctions were disrupted due to lack of attachment by the intermediate filament bundles (Bornslaeger, Corcoran, Stappenbeck, & Green, 1996). Other studies suggested that loss of DP by 50% is still sufficient for normal development and function in non-palmoplantar skin but is insufficient to maintain normal adhesion function in the skin of palms, and soles (Thomason, Scothern, McHarg, & Garrod, 2010).

2.2.4 Functions of DSMs

The primary functions of DSMs are to mediate cell to cell adhesion and maintain tissue integrity (Garrod & Chidgey, 2008). DSMs provide a scaffold for anchoring the keratin intermediate filaments to the plasma membrane, and act as signaling centers (Brown & Wan, 2015). Different expression patterns of the desmosomal cadherins (DCs) in epidermis indicate DSMs are biochemically and functionally distinct at various layers of the tissue (Delva, Tucker, & Kowalczyk, 2009).

Studies suggest DSMs function beyond mechanical adhesion. For instance, one study showed that Dsg1 is able to suppress the epidermal growth factor receptor induced mitogen activated protein kinase signaling (EGFR-MAPK) during the process of epidermal differentiation, except for its extracellular adhesion function

(Getsios et al., 2009). Also, Dsc2 was identified to be involved in the activation of the Akt- β catenin signaling pathway in the progression of colorectal cancer (Kolegraff, Nava, Helms, Parkos, & Nusrat, 2011). Another interesting study showed that loss of either Dsg1 (Johnson et al., 2014) or Pg (Dusek et al., 2007) delays the programmed cell death in response to UV treatment, suggesting that these proteins play a pro-apoptotic signaling role in the skin. All these studies suggest that desmosomal proteins transcend their roles in mechanical adhesion and contribute to intracellular signaling in a wide variety of biological processes (Dubash & Green, 2011).

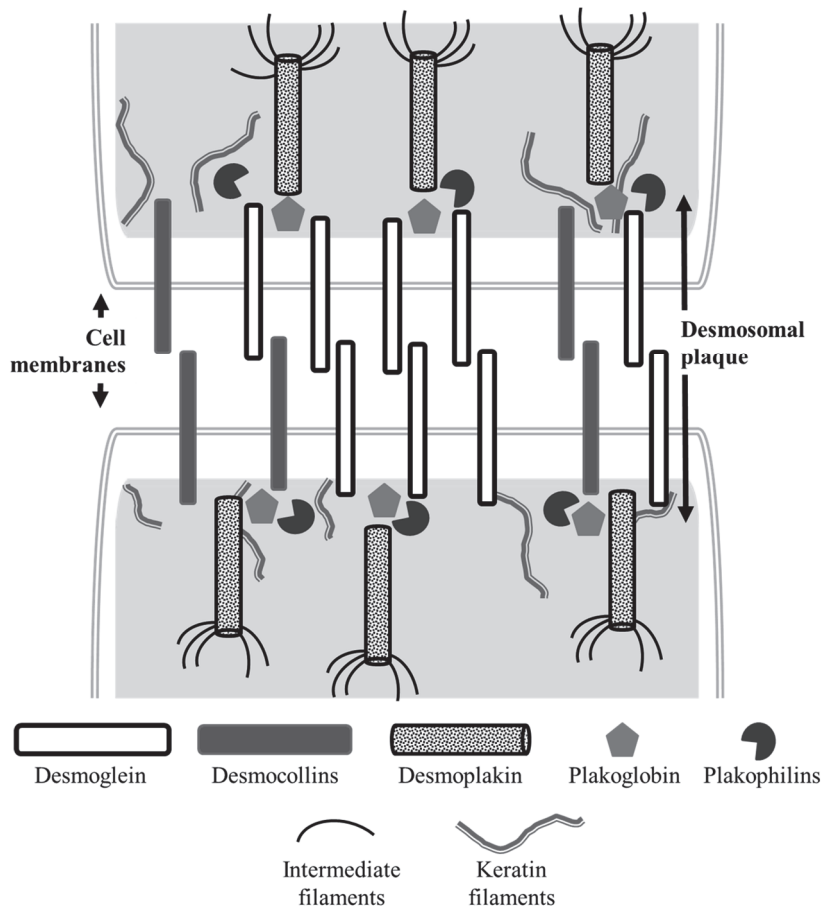


Fig. 1. Schematic model of a desmosome with relative positions of the major desmosomal components. The illustration was drawn according to (Brooke, Nitoiu, & Kelsell, 2012) after modifications.

2.3 Desmoglein 3 (Dsg3)

Desmoglein 3 (Dsg3) is a 130 kDa transmembrane glycoprotein which plays a role in epithelial cell-cell adhesion. As a member of the desmoglein subfamily it belongs to the cadherin superfamily. Dsg3 is best known as the pemphigus vulgaris antigen since it was identified as a major auto-antigen in this disease (Fukuoka et al., 2007). Dsg3 expression is restricted to the basal and immediate suprabasal layers of the skin. However, in the oral mucosa, Dsg3 is uniformly expressed throughout the stratified epithelium (Tsang et al., 2012).

2.3.1 Dsg3 structure

The structure of the Dsg3 protein is shown in Figure 2. The extracellular (EC) domain can be subdivided into four cadherin like EC domains and extracellular anchor (EA) domain. Its cytoplasmic tail consists of an intracellular anchor (IA), and an intracellular cadherin specific (ICS) domain. This ICS domain has a specific binding site for Pg. Other domains found in Dsg3 cytoplasmic tails are an intracellular proline-rich linker (IPL) domain, a repeat unit domain (RUD) and a glycine rich desmoglein terminal domain (DTD) (Lee et al., 2009).

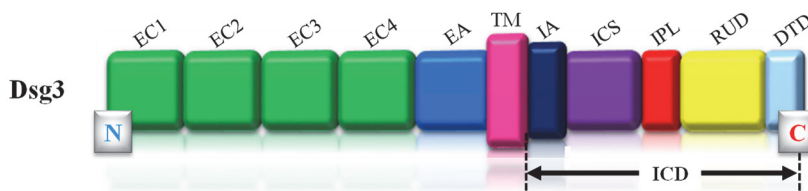


Fig. 2. Schematic illustration of the structure of Dsg3. It consists of four extracellular cadherin like repeats (EC1-EC4), an extracellular anchoring domain (EA), a transmembrane domain (TM) and a cytoplasmic tail. The cytoplasmic tail includes an intracellular anchoring domain (IA), intracellular cadherin specific domain (ICS), proline rich linker domain (IPL), a repeat unit domain (RUD), glycine rich terminal domain (DTD), C-terminal end (C) and N-terminal end (N). The illustration was drawn according to (Lee et al., 2009) with some modifications.

2.3.2 Dsg3 signaling

Many intracellular signaling pathways are involved in maintaining standard cellular functions and homeostatic environment. These pathways transmit information within the cell. Dsg3 proteins are involved in maintaining, regulating cell proliferation and differentiation by triggering these pathways (Garrod & Chidgey, 2008). A study based on RNA interference, in HaCat keratinocytes and MDCK cell lines, showed that Dsg3 silencing resulted in cell-to-cell adhesion defects concomitant with decreased cell proliferation, and impaired skin regenerative ability. These findings directed that Dsg3 has a role in controlling cell proliferation and tissue regeneration by regulating cell-cell, and DSMs adhesion (Mannan et al., 2011).

Src family proteins are non-receptor tyrosine kinases. They are involved in AJ protein turnover and regulating cellular responses. Studies have shown Dsg3 involvement in activating Src signaling via interaction with E-cadherin. Studies based on gain and loss of function approaches in various cell lines show that Dsg3 can act as a positive upstream regulator of Src activity, which in turn helps to mediate AJ formation (Tsang et al., 2010). Because of the abnormally enhanced Src activity in response to overexpression of Dsg3, the cells also exhibited pronounced membrane projections and accelerated cell migration in human oral buccal SCC SqCC/Y1 cells (Tsang et al., 2010). A later report by the same group (Tsang, Brown, Gadmor et al., 2012) provided direct evidence that non-junctional Dsg3, which associates with E-cadherin, directly regulated Src signaling during junction formation. They also showed that this pathway is likely involved in the pathogenesis of pemphigus vulgaris based on the evidence that decreased pSrc signaling accompanied loss of E-cadherin in the basal keratinocytes surrounding the blisters (Tsang et al., 2012).

2.3.3 Dsg3 in disease

Dsg3 is the pemphigus vulgaris (PV) antigen

The autoimmune disease pemphigus vulgaris (PV) occurs due to loss of cell to cell adhesion and blister formation. It is a disease caused most probably by circulating antibodies directed against Dsg3. The presence of antibodies against both Dsg3 and Dsg1 can cause mucocutaneous disease with blisters present in the deep mucosa or epidermis (Ruocco et al., 2013). The loss of cell to cell adhesion is called

acantholysis. Many studies have shown that binding of the autoantibodies to Dsg3 triggers a cascade of intracellular events that may contribute to the pathophysiology of pemphigus vulgaris (Tsang et al., 2012). At the early stage of PV, anti-Dsg3 antibodies are found in patients who suffer from mucous membrane lesions, but sera containing both anti-Dsg3 and anti-Dsg1 are detectable in patients with lesions involving more than just the mucous membranes. Studies have found that autoantibodies recognizing the Dsg3 epitopes at the amino terminal domains play a major role in the pathology of disease (Tsunoda et al., 2003; Amagai et al., 1995). Aoyama and Kitajima (1999) proposed that pemphigus vulgaris is caused by atypical desmosomes, which lack Dsg3, since human skin SCC cells *in vitro* treated with pemphigus vulgaris antibodies did not contain Dsg3 (Aoyama & Kitajima, 1999).

Dsg3 in cancer

In squamous cell carcinoma (SCC), Dsg3 is overexpressed compared to normal epithelium (Fukuoka et al., 2007). Dsg3 can be used as a specific marker for head and neck SCC staging (T, N & overall stage). However, its biological function in cancer metastasis remains unknown. RNAi knockdown of Dsg3 in OSCC cell lines inhibited cell growth, migration and invasion. This suggests an additional role of Dsg3 in cancer (Chen et al., 2007). Additionally, Dsg3 knockdown showed an effect on OSCC cell growth and invasion, by enhanced Pg interaction with the transcriptional factor TCF and quenched TCF/LEF transcriptional activity (Chen et al., 2013). We showed that Dsg3 promotes cancer cell migration and invasion through regulatory mechanisms of the transcriptional factor AP-1 and the FERM protein ezrin (Brown et al., 2014). Another report has revealed the possibility to adopt Dsg3 as a prognostic biomarker for lymph node metastasis in head and neck SCC (Patel et al., 2013).

2.3.4 Dsg3 as an anti-cancer drug target

Dsg3 has been proposed as a possible therapeutic target in OSCC. Chen et al. showed that RNAi mediated Dsg3 silencing in OSCC cell lines suppressed tumor growth and metastasis in xenografts of BALB/C nude mice (Chen et al., 2007; Chen et al., 2013). This suggests the therapeutic potential of targeting Dsg3 to prevent cancer progression. In another study, a panel of anti-mouse Dsg3 IgG mAbs using Dsg3 knockout (-/-) mice immunized with recombinant mouse Dsg3 (AK series of

mAbs) was generated (Tsunoda et al., 2003). These mAbs mapped to different regions of the extracellular domain of mouse Dsg3 (mDsg3) and among them, the mAb AK23 was characterized as a pathogenic antibody which recognizes the N-terminal adhesive epitope on mDsg3.

Although the effects of these antibodies on cell-cell adhesion have been addressed, their role on cell migration is unknown. Currently, three of these mDsg3 AK series of antibodies are commercially available (AK23, AK9, and AK18), and only AK23 cross-reacts with the EC1 domain of human Dsg3 (Di Zenzo et al., 2012). AK23 has been used to study pemphigus blister formation, but there is very little known about targeting Dsg3 to inhibit carcinoma cell migration and invasion (Brown & Wan, 2015).

2.3.5 Expression of Dsg3 C-terminally truncated proteins and their dominant negative effect on cell-cell adhesions

In previous biomedical research, the functions of Dsg3 were studied using one or a combination of *in vitro* and *in vivo* model systems. For example *in vitro*, primary tumor and their derived cancer cell lines were studied with Dsg3 up-regulation or knockdown, and also *in vivo* models were examined with Dsg3 knockout, or transgenic animals with misexpression or the expression of its N-terminally truncated mutant in epidermis (Allen, Yu, & Fuchs, 1996; Baron, Hoang, Vogel, & Attardi, 2012; Chen et al., 2013; Merritt et al., 2002). In addition, there are studies based on IgGs from PV patients (Amagai, Klaus-Kovtun, & Stanley, 1991; Payne, Hanakawa, Amagai, & Stanley, 2004) and the active pemphigus disease model in which pathogenic antibodies specific for Dsg3 are raised (Amagai, Tsunoda, Zillikens, Nagai, & Nishikawa, 1999; Jennings et al., 2011).

The methodologies used to examine the protein function *in vitro* fall into two categories: 1) a gain-of-function approach achieved through the overexpression of target gene(s) or the constitutive activation of the protein through a gain of function mutation; 2) a loss-of-function approach achieved through either target gene silencing by RNAi or the expression of a dominant negative mutant to reduce or abolish the endogenous protein function. All of the mentioned techniques have their merits and demerits as the manipulation of cellular genetic material, protein structure and expression may have biological effects not directly pertaining to the protein of interest resulting in misleading observations. Through experimenting combination of gain- and loss-of-function approaches, one can compensate for some of the limitations of a single model for the study of protein function.

Although the evidence of cross-talk between Dsg3 and E-cadherin has been observed in previous studies (Rotzer et al., 2015; Tsang et al., 2010), it remains obscure how Dsg3 regulates E-cadherin function. For instance, it remains unclear whether Dsg3 is only involved in the E-cadherin junction assembly at an early stage of junction formation, or is it also required for the maintenance of E-cadherin associated adhesion or both. Since these junctions are highly dynamic complex structures, a detailed study on their reciprocal influence on protein synthesis and turnover is still lacking.

There was no clinical evidence of Dsg3 truncated mutations in human diseases till most recently, a homozygous nonsense mutation in the Dsg3 gene has been identified in human and for the first time, that causes recurrent blisters, and erosion in oral mucosa of a one-year-old female baby (Kim et al., 2018). In addition, three mouse models have been developed by targeted disruption of the Dsg3 gene (Pulkkinen et al., 2002). Both mice mutants, *Dsg3^{bal-2J}* and *Dsg3^{tm1stan}*, presented runting and a hair loss phenotype (Davisson, Cook, Johnson, & Eicher, 1994; Koch et al., 1997; Montagutelli et al., 1997). Another mouse mutation, *Dsg3^{bal-Pas}*, had similar clinical features, including runting and hair loss, and it exhibited fragile skin and oral mucous membranes (Montagutelli et al., 1997).

2.4 Tumor microenvironment (TME)

Tumors are surrounded by extracellular matrix (ECM) and stromal elements; these cellular and noncellular components of the tumoral niche form the tumor microenvironment (TME) (Wang et al., 2017). The TME plays an active role in cancer progression. ECM components, different cells, microvasculature, interactions between cancer cells and matrix molecules have an influence on tumor enlargement and invasion (Gkretsi, Stylianou, Papageorgis, Polydorou, & Stylianopoulos, 2015). Due to modifications in surrounding environmental conditions and oncogenic signals from growing tumors, the TME gradually changes over the course of cancer progression and modulates cancer cell migration and invasion (Quail & Joyce, 2013).

2.4.1 Composition of TME

The TME consists of non-cancerous cells [such as inflammatory cells, vascular cells, and carcinoma-associated fibroblasts (CAFs)], matrix molecules (i.e., collagen, laminin and fibronectin), enzymes [matrix metalloproteinases (MMPs)], growth factors [such as epidermal growth factor (EGF), platelet derived growth factor (PDGF), and fibroblast growth factor (FGF)] and cytokines [interferon-gamma, interleukins (IL) 2, 4, 10, and 12] (Fig 3). TME components interact with each other and also affect cancer cell proliferation, invasion and metastasis formation (Ansell & Vonderheide, 2013; Mocellin, Wang, & Marincola, 2001; Salo et al., 2014; Salo et al., 2018; Zhang, Nie, & Chakrabarty, 2010).

2.4.2 Role of TME in cancer progression

The ECM components of the TME have an active role in cancer invasion during different stages of tumor progression. The ECM scaffolds TME components and modulates cancer cell spreading, as well as cell movement. Key ECM factors such as growth factors and chemokines provide strength, and elasticity to the tissues (Balkwill, Capasso, & Hagemann, 2012). During the primary stages of cancer growth, genetic changes occur which trigger various mechanisms controlling the secretion of these various growth factors, ECM proteins, and cytokines. These secretions change, also transform ECM and TME into pro-tumorigenic shape. Through various components and secreted factors, the TME has an active role in controlling the hallmarks of cancer (Hanahan & Weinberg, 2011).

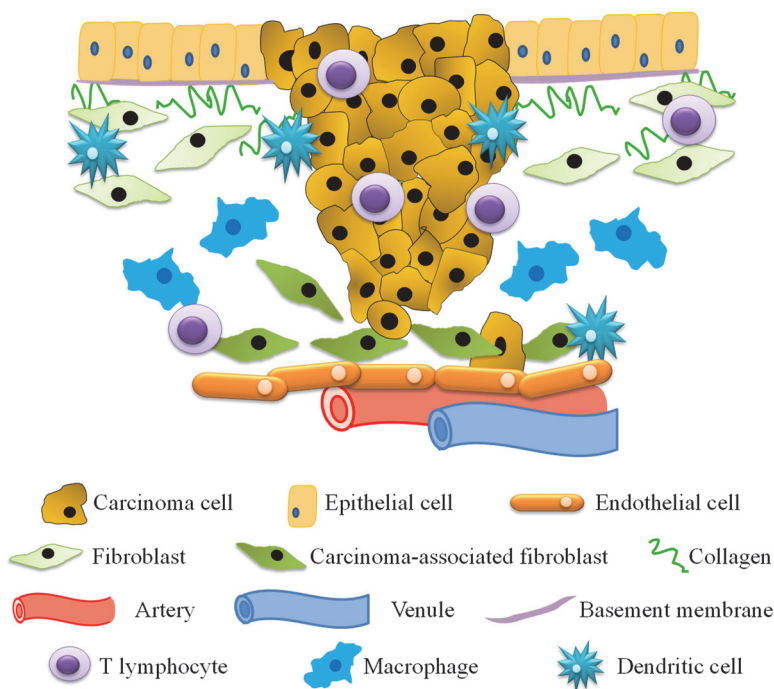


Fig. 3. Composition of the tumor microenvironment. The TME contains fibroblasts, carcinoma-associated fibroblasts, inflammatory cells, vessel structures, extracellular matrix molecules, and soluble factors. This simple illustration was drawn according to (Joyce & Pollard, 2009) with some modifications.

Major TME components (both cellular and acellular), including inflammatory cells, CAFs, extracellular vesicles (EVs) and various soluble factors, and matrix structural molecules modulate the dynamic course of cancer cell migration, invasion and metastasis (Joyce & Pollard, 2009; Salo et al., 2018). Different key ECM proteins including laminin and type IV collagen control the cancer cell-stroma interactions (Salo et al., 2014). In addition, in OSCC progression, laminin-332, type IV collagen and fibronectin show increased expression (Kulasekara et al., 2009). Other key ECM molecules, such as Tenascin-C (TNC) also has an important role in regulating OSCC invasion (Berndt, Richter, Kosmehl, & Franz, 2015; Sundquist et al., 2017). Cellular components of the TME modulates OSCC invasion, such as immune cells like macrophages (Pirila et al., 2015), mesenchymal stem cells (Sobral et al, 2011; Salo et al, 2013), and CAFs (Dayan et al., 2012; Sundquist

et al., 2016). Studying different TME components give an insight into its role in cancer progression and anti-cancer drug therapy (Salo et al., 2014).

2.4.3 TME matrices

In research, the TME has been mimicked using different matrices and 3D *in vitro* methods. The popular methods for studying cancer cell invasion include embedding cancer cells within rodent tissue derived Matrigel[®] and collagen. Other mimicking gels such as fibrin, hyaluronic acid, chitosan, alginate, or silk fibrils are also used for 3D cell culture. However, they are less effective at promoting 3D culture than Matrigel[®] (Fang & Eglén, 2017).

Both Matrigel[®] and collagen are used commonly in wound healing assays, Transwell invasion assays, 3D spheroids (Justus, Leffler, Ruiz-Echevarria, & Yang, 2014; Kramer et al., 2013) and sandwich cultures (Akerfelt et al., 2015). However, these matrices do not simulate the human TME matrix (TMEM) because of their rodent origin. It has been shown that mouse and human tissues vary in composition; mouse TME has, for example, 75 more proteases than human (Puente, Sanchez, Overall, & Lopez-Otin, 2003). Therefore, there is a concern of misrepresentation of the experimental results using these animal tissue-based models in human cancer related experiments. In order to overcome these difficulties our research group introduced a 3D *in vitro* invasion model using discs of human uterine leiomyoma tissue (Nurmenniemi et al., 2009). A myoma disc mimics the human TME *in vitro* more accurately than animal derived matrices for cultured solid cancer cells.

Matrigel[®]

Matrigel[®] is a gelatinous protein mixture produced from the Engelbreth-Holm-Swarm (EHS) mouse sarcoma tumor (Hughes, Postovit, & Lajoie, 2010). The name, EHS tumor was to honor the Danish scientist who discovered it, J. Engelbreth-Holm, and Richard Swarm, who was responsible for its maintenance and characterization (Kleinman & Martin, 2005).

Matrigel[®] has a heterogeneous composition, containing ECM proteins such as laminin, nidogen, collagen, and heparan sulfate proteoglycans. Matrigel[®] also contains various growth factors (transforming growth factor beta, epidermal growth factor, fibroblast growth factor, etc) (Benton et al., 2011; Hughes, Postovit, & Lajoie, 2010). Matrigel[®] is routinely used in different 3D *in vitro* invasion and clonogenic assays and 3D cultures (Benton et al., 2011).

Collagen

Collagen is a major ECM component that has been widely used for *in vivo* mimicking conditions to facilitate cellular growth and differentiation. It interacts with cells and growth factors, and has a chemotactic action over endothelial cell behavior (Chan et al., 2016). In vertebrates, 28 types of collagen (I–XXVIII) have been identified, which can be divided into fibrillar, and non-fibrillar forms (Ricard-Blum, 2011). Due to its biological, mechanical and degradable properties, collagen is widely used in many experimental procedures, including clinical applications (Abou Neel et al., 2013; Yannas, Tzeranis, Harley, & So, 2010).

Collagen-based biomaterials can also provide the required cellular scaffolds for tissue repair and regeneration (Chan et al., 2016). Scaffolds made of collagen can support physiological processes in the course of healing and provide a platform for the development of ideal 3D tissue models (Chan et al., 2016). Commercially available rat tail tendon derived type I collagen, is the most commonly used collagen in cell biology studies. Organotypic models with type I collagen together with mouse EHS sarcoma-derived Matrigel[®], collagen-Matrigel[®] mixtures, are used for invasion studies of carcinoma cells (Anguiano et al., 2017).

Fibrin

Fibrin gel can be derived from human fibrinogen. Fibrin is an effective component of the fibrinogen gel that can enhance angiogenesis via activating angiogenic growth factors such as vascular endothelial growth factor (Morin & Tranquillo, 2013; Shiose et al., 2004). At most injured locations, fibrin is activated by enzymatic polymerization of fibrinogen. In wound healing and cell migration, fibrin is reorganized and degraded by enzymatic functions of cells. Combined with various ECM components (fibronectin, vitronectin, laminin, and collagen), fibrin gels can further enhance their activity (Schense & Hubbell, 1999).

Various studies have revealed that fibrin can be used in medical and bioengineering research, due to its biochemical and mechanical properties (Janmey, Winer, & Weisel, 2009). Human cells such as fibroblasts can normally spread and proliferate in fibrin gels *in vitro* (Zhao et al., 2008). In skeletal muscle and cardiac tissue engineering applications, fibrin gel has been used as a hydrogel (Chan et al., 2016).

2.4.4 Three dimensional (3D) TME matrix models

Conventional cancer cell studies have focused primarily on 2D *in vitro* models. Although these explain the mechanical details of cell-substrate or cell-cell interactions, they are inadequate to investigate *in vivo* like cell-matrix interactions (Friedl & Brocker, 2000; Rangarajan & Zaman, 2008). *In vitro* 3D TME culture models cover the gap between 2D culture and *in vivo* models (Harjanto & Zaman, 2013; Shamir & Ewald, 2014), in that they resemble closely the matrix structure and rheology surrounding cancer cells in nature (Katt et al., 2016; Zaman et al., 2006). One significant biophysical parameter is storage modulus or stiffness, which allows the ECM to resist deformation and modulates cancer cell-cell adhesion, migration, and invasion (Wells, 2008; Wolf & Friedl, 2011). The limited availability of high quality *in vitro* 3D TME models is an obstacle to obtaining large amounts of accurate cell migration data for analysis. (Rangarajan & Zaman, 2008). Time-lapse microscopy with fluorescently labeled cells is used to track trajectories, which enable quantitative analysis of different parameters such as cell velocity/speed and nuclear size within the 3D matrix (Katt et al., 2016; Zaman et al., 2006). Various 3D *in vitro* TME models are used to study cancer cell invasion, such as transwell invasion model, spheroid model, hanging drop, 3D sandwich, and myoma organotypic model, etc.

Transwell invasion

The transwell invasion assays are probably the most commonly practiced invasion model, which are based on the original Boyden assay system (Marshall, 2011). It is used to analyze the characteristics of cancer cells to directionally respond to various chemoattractants (Justus, Leffler, Ruiz-Echevarria, & Yang, 2014). To recapitulate the exact TME, an ECM layer is placed on the porous membrane (Fig 4). Commonly used ECM matrices are typically Matrigel[®] (Marshall, 2011) and collagen (Katt et al., 2016). The thickness of the matrix layers can reach up to 1 mm (Kramer et al., 2013). Invasive cells degrade and move through the ECM layer and adhere to the bottom of the filter, and then their invasiveness is analyzed.

3D hanging drop

This simple method generates tissue-like cellular aggregates for measuring biomechanical properties or for molecular analysis in a physiologically relevant

model (Foty, 2011). Small droplets (15-20 μl) of fluorescently labeled cancer cells are embedded in different matrices (Salo et al., 2015). Cell suspension in matrix drops is placed in the centers of each compartment on the inner side of a four-compartment culture plate lid. This allows the cells to come close to each other with gravitational support (Fig 5A). After a short incubation, the plate is gently inverted and placed inside the incubator for another 3 hours. In this way, the cells will spread before the matrix polymerizes. Time-lapse imaging up to 20-24 hours is completed later using a confocal fluorescence microscope. The images obtained can then be processed, segmented and analyzed by available image analysis software. Different cell invasion parameters such as cell speed, cell volume and shape (roundness/ eccentricity) can be analyzed.

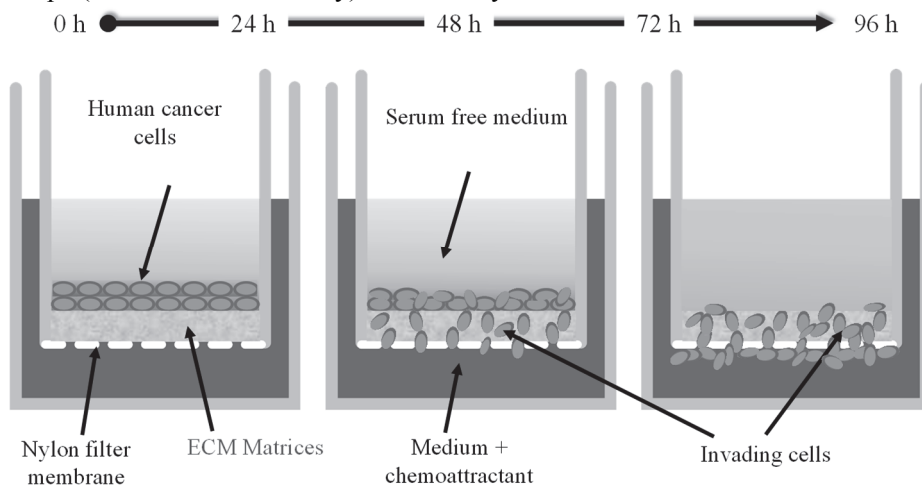


Fig. 4. Transwell invasion model with ECM coatings.

3D spheroid model

Cancer spheroids or multicellular tumor spheroids (MCTS) can be defined as aggregates of cancer cells grown in suspension and imbedded within TME matrices using 3D culture models (Fig 5B). 3D spheroids are used for functional studies (e.g., cell growth, migration, and invasion) in an avascular TME, drug testing, angiogenesis studies, tumor-immune cell or tumor-CAF interaction studies (Katt et al., 2016; Lin & Chang, 2008; Mehta et al., 2012). Four techniques are used for spheroid formation, such as suspension culture, hanging drop, microfluidic, and non-adherent surface methods (Mehta et al., 2012). Suspension cultures form

spheroids through agitation or by increasing the viscosity of the media. It has high throughput, but there is no guarantee of proper size and uniformity (Lin & Chang, 2008; Mehta et al., 2012).

The hanging drop method where cancer cell droplets are suspended from the underside of a tissue culture lid allows better control of spheroid size and composition. Gravity drives mechanical cell aggregation into a cluster at the bottom of the drop and forms a spheroid. Then spheroids are imbedded into a TME matrix mixture (Salo et al., 2015). This technique provides uniform spheroid size, and for co-culture spheroid models, as it allows natural cell-cell interactions (Mehta et al., 2012). Cancer cells cultured on non-adherent or ultra-low attachment surfaces don't attach to the substrate, which allows spheroid formation. Using non-adherent surfaces is straightforward but does not allow control over spheroid size and uniformity (Mehta et al., 2012). Spheroid growth can be modified using round-bottom non-adherent 96-well plates (Vinci et al., 2012). Microfluidic devices are now common, as they allow controlled spheroid formation. Persistent perfusion under physiological conditions during spheroid formation allows for rapid formation and more uniformity (Mehta et al., 2012).

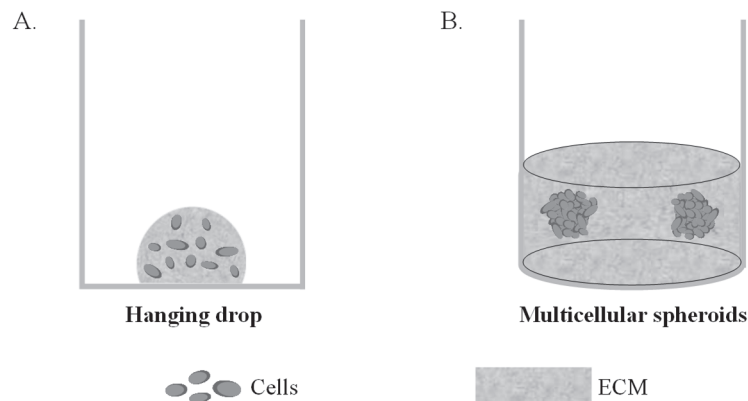


Fig. 5. Cancer cells embedded in TME matrices. A. Hanging drop technique. B. Multicellular spheroid model.

3D sandwich

Here fluorescent-labeled cancer cells are imbedded between two layers of polymerized 3D TME matrices (Fig 6). This mimics the environment of the cells

within a tissue and allows cells to be imbedded in a narrow focal plane between two layers of ECM (sandwich), which is ideal for long term imaging. This 3D culture method is performed in 96-well angiogenesis plates (Ibidi) featuring a well-in-a-well geometry consisting of two compartments (inner smaller & upper larger). The inner well is filled with gel matrix. After cells are placed on top of the polymerized gel, the upper well is filled with the same gel matrix so that the cells are allowed to grow and move between two layers of ECM (Harma et al., 2014). Quantification of invasion and morphological changes can be made using fluorescently labeled cells and co-culture with fibroblasts (Akerfelt et al., 2015). It is ideal for better visualization without any meniscus formation caused by liquid tension and with all cells in one focal plane.

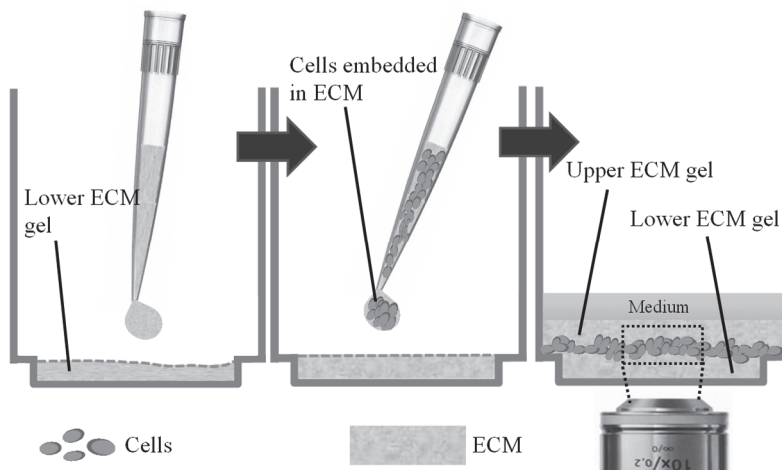


Fig. 6. Sandwich culture, where single cells or spheroids are imbedded between two layers of ECM.

Myoma organotypic model

Our research group introduced a uterine leiomyoma tissue based myoma model to overcome the lack of human tumor mimicking TME matrices in 3D *in vitro* invasion assays (Nurmenniemi et al., 2009). It contains several insoluble as well as soluble molecules (e.g. laminins, type I, II, and IV collagens) and presents more of the different kinds of cells and molecules present in the natural TME compared to the previous *in vitro* models (Sundquist et al., 2016; Nurmenniemi et al., 2009; Teppo et al., 2013). Here cancer cells are cultured on top of the myoma disc, then

they invade into the myoma tissue (Fig 7). Briefly, myoma tissue is cut into 4 mm myoma slices, later the myoma discs are cut using an 8 mm biopsy punch. Then the discs are transferred carefully to a disc inside a Transwell chamber, cells are counted and placed on top of the center of discs. Each disc is transferred from the Transwell chamber onto a metallic grid and cultured in a 12-well plate for 10-14 days. Later the discs are fixed with 4% formalin and processed prior to hematoxylin and eosin staining or pan-cytokeratin AE1/AE3 immunohistochemical staining. High-quality images from the stained sections can be collected by a DMRB photo microscope, and various parameters, such as invasion area, and invasion depth are measured by Fiji or available software (Astrom, Heljasvaara, Nyberg, Al-Samadi, & Salo, 2018).

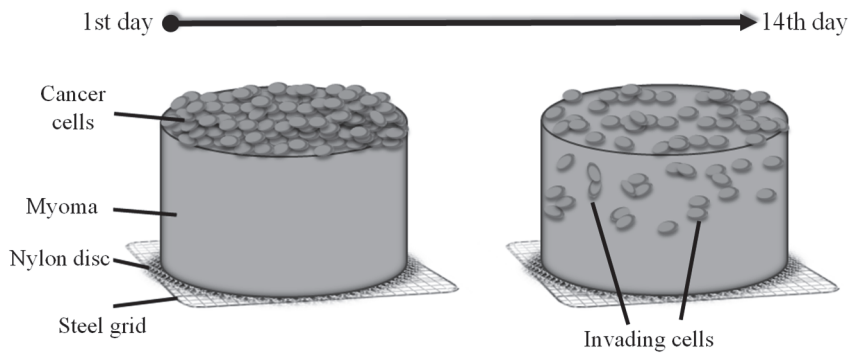


Fig. 7. Schematic drawing of myoma invasion model.

3 Aims of the present study

The main aims of the present study were:

1. To study the role of Dsg3 in adhesion, migration, and invasion *in vitro* by utilizing both gain and loss-of-function approaches of Dsg3 in buccal mucosa SCC cell lines (I, III).
2. To compare the effects of locally established human leiomyoma derived matrices (myoma discs and Myogel) with commercial rodent matrices (Matrigel[®] and type I collagen) (II, III).
3. To compare the adhesion and invasion properties of oral mucosal SCC cell lines in different matrices in 3D models (II, III).
4. To explore the feasibility of using Dsg3 as a potential novel anti-cancer drug target (III).

4 Materials and methods

The materials and methods used in the original articles are summarized in Table 2. The most important methods of the present thesis are briefly described below.

Table 2. Methods used in the original publications.

Level	Method	Publication
Human	Myogel	II, III
	Myoma organotypic disc	III
Animal models	Mouse sarcoma derived Matrigel®	II, III
	Rat tail tendon derived type I collagen	II, III
Cells	Cell culture	I, II, III
	Cell co-culture	III
	Establishment of stable transfected HSC-3 (GFP-H2B) cells	II
	Establishment of stable transfected SqCC/Y1 (H2B) cells	III
Cell experiments	Establishment of stable transfected CAFs (GFP)	III
	Soft agar colony formation assay	II
	Migration assays	II, III
	Transwell Vertical migration	II, III
	Horizontal migration	III
	Invasion assays with tissue derived gels	II, III
	Transwell vertical invasion	III
	3D Sandwich assay	III
	3D Hanging drop assay	II
	3D Multicellular spheroid assay	II
Histological experiments	Invasion assays with tissue discs	III
	3D Myoma organotypic assay	III
Protein analyses	Cell death assay (TUNEL)	II
	Immunofluorescence (IMF)	I, III
Microscopic techniques	Staining and analysis of immunohistological samples	III
	Adhesion assay	III
	Confocal microscopy	I, II, III
	Live-cell imaging	II, III
Image analysis softwares	IncuCyte™ (Essen BioScience, United Kingdom)	III
	Spinning disc confocal microscope (Carl Zeiss, Germany)	II
	Epifluorescence microscope (Olympus, Japan)	III
Others	Fiji ImageJ (NIH, Bethesda, USA)	I, II, III
	MetaMorph (Molecular Devices Corp, USA)	III
	MATLAB (MathWorks, USA)	II, III
Others	Matrix rheology measurement	III
	Statistical analyses	I, II, III

Table 3. Antibodies used in the original publications.

Antibodies (Abs)	Name	Source	Dilution	Publication
<i>Primary</i>	Mouse anti-Dsg3 Ab, 5H10	Prof M Amagai	1:100	I
	Mouse anti-E-cadherin Ab, HECD-1	Abcam, UK	1:100	I
	Rabbit Ab, H145	Santa Cruz, USA	1:100	I
	Rabbit Myc-Tag Ab	Cell Signaling, USA	1:50	I
	Alexa Fluor 488/568, Goat anti-mouse (green/ red)	Invitrogen, USA	1:100	I
<i>Secondary</i>	Alexa Fluor 488, Goat anti-mouse (green)	Invitrogen, USA	1:100	I
	Alexa Fluor 488, Goat anti-mouse (green)	Invitrogen, USA	1:100	I
	Alexa Fluor 488, Goat anti-rabbit (green)	Invitrogen, USA	1:100	I
	Anti-rabbit (red/ green)	Invitrogen, USA	1:100	I
	Anti-Desmoglein 3 (Mouse) mAb (AK23)	MBL, Japan	1 µg/ ml	III
<i>Other</i>	Mouse IgG1	MBL, Japan	1 µg/ ml	III
	Cytokeratin (AE1/AE3)	Dako, Denmark.	1:250	III

4.1 Cell cultures (I, II, III)

4.1.1 Carcinoma cell lines and their characteristics (I, II, III)

SqCC/Y1 cells derived from human oral buccal SCC were used for the study (I, III) and they were grown in EpiLife medium with 60 mM calcium concentration (Gibco) supplemented with EDGS (EpiLife Defined Growth Supplement, Gibco). Four different SqCC/Y1 cell lines were generated in Dr. Hong Wan's research laboratory in Queen Mary University of London, with the transduction of vector control (Ct), full-length (FL) or two different C-terminally truncated Dsg3 mutants (Δ 238 and Δ 560) (Fig 8) as described (Moftah et al., 2016). In brief, a retroviral construct of

full-length (FL) human Dsg3 cDNA tagged with a Myc epitope at the C-terminus (pBABE-hDsg3.myc), was generated during our earlier study (Tsang et al., 2010). Two mutants (Fig 8) were produced by cutting out different length sequences in the pBABE-hDsg3.myc construct (I). Two Abs against Dsg3, mAb 5H10 directed to the N-terminal end and rabbit anti-Dsg3 directed to the C-terminal end, were used for the protein expression analysis. Although little or no reduction in total endogenous Dsg3 expression was detected in cell lines with transduction of mutants by Western blot analysis, disruption of cell-cell junctions with concomitantly compromised adhesion strength was shown in these cell lines (I).

The human OTSCC cell line HSC-3 (Japan Health Sciences Foundation, Japan) was cultured in a 1:1 DMEM/F-12 medium (Life Technologies) supplemented with 100 U/ml penicillin, 100 µg/ml streptomycin, 250 ng/ml fungizone, 50 µg/ml ascorbic acid and 0.4 µg/ml hydrocortisone (all from Sigma-Aldrich) and 10 % heat inactivated fetal bovine serum (FBS; Life Technologies) (II).

4.1.2 Other cell lines (III)

Human carcinoma-associated fibroblasts (CAF) and normal oral fibroblasts (NOF) were established from OSCC or healthy oral mucosa respectively, as described earlier (Sobral et al., 2011). Both cell lines were cultured in DMEM medium supplemented with 100 U/ml penicillin, 100 µg/ml streptomycin, 50 µg/ml ascorbic acid, 250 ng/ml fungizone, 1 mmol/L sodium pyruvate (Sigma-Aldrich) and 10 % heat inactivated FBS.

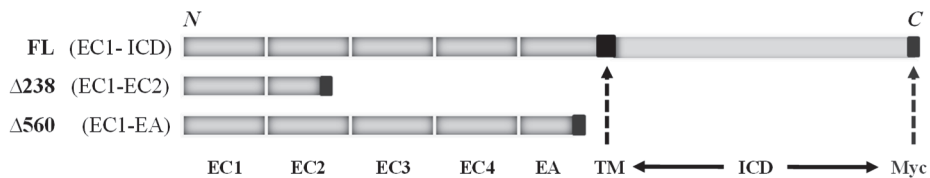


Fig. 8. Full-length and mutant forms of Desmoglein 3 (Dsg3). A schematic diagram of full length (FL) and two C-terminally truncated mutants ΔC ($\Delta 238$ and $\Delta 560$) of Dsg3 tagged with myc epitopes (red) are drawn according to (I). Abbreviations: EC: extracellular domain; EA: extracellular anchorage domain; TM: transmembrane domain; ICD: intracellular domain; C: C-terminal end; N: N-terminal end.

4.2 Lentiviral transduction (II, III)

SqCC/Y1 and HSC-3 cell lines were transduced with nuclear histone-2B (H2B) - coupled mCherry expression vector pLenti6.2 V5/DEST (a kind gift from Dr. Cindy E. Dieteren, Radboud UMC, Netherlands) following a published protocol and selected in culture media containing 5 µg/ml blasticidin-S (Merck Millipore) (Cattavarayane, Palovuori, Tanjore Ramanathan, & Manninen, 2015). CAFs and HSC-3 cells labeled with GFP were generated by stable transduction with nonsilencing GIPZ lentiviral shRNAmir control particles (pGIPZ vector contains GFP in order to track shRNAmir expression; Thermo Fisher Open Biosystems) and selected with 4 µg/ml puromycin (Sigma-Aldrich) according to the manufacturer's instructions. Transduced SqCC/Y1-H2B, HSC-3 (H2B-GFP) and CAF-GFP cell lines were later cultured as their non-transduced counterparts.

4.3 Dispase dissociation assay (I)

The dispase dissociation assay was carried out to study cell-cell attachment in SqCC/Y1 cell lines, according to previously described methods with modifications (Hartlieb et al., 2013; Mannan et al., 2011). Cells were counted and placed in 6-well plates, and were cultured to confluency in EpiLife medium with EDGS. Then, confluent cultures were gently washed twice with PBS, later incubation was done in 2 ml dispase II (2.4 U/ml in PBS, Invitrogen) for 20-30 minutes. Incubation was carried out till whole epithelial sheet loosened from the plate substrate. Mechanical stress was then applied by gentle pipetting 5 times with 1 ml pipette to fragment the epithelial sheets. After the epithelial sheets detached, images of each well were taken, and then the number of fragments in each well was determined by counting the number of particles after thresholding with ImageJ.

4.4 Immunofluorescence (I, III)

For immunofluorescence (IMF) studies the reagents used were as follows: fixative – ice cold methanol, washing buffer (PBS plus 0.2% Tween 20), blocking buffer (10% goat serum in washing buffer), primary and secondary antibodies (Abs) (Table 3) and DAPI. SqCC/Y1 cells grown on coverslips were washed with PBS, fixed in ice-cold methanol and rehydrated. Next, the coverslips were incubated in the primary antibody and secondary antibody, then counterstained with DAPI for at least 10 minutes at room temperature (RT). IMF procedures were carried out as

described in (Moftah et al., 2016). All coverslips were mounted on the labeled slides using ProLong® Gold antifade reagent (Catalog Number- P36931, Invitrogen). The coverslip staining was examined with a Leica DM5000 epifluorescence microscope. Image analysis was performed using ImageJ.

4.5 Horizontal migration (III)

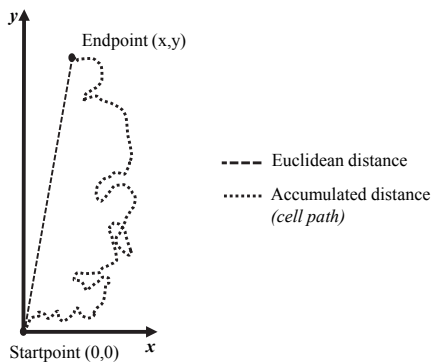
An IncuCyte™ Live-Cell Imaging System (Essen Bioscience) was used for 2D migration imaging. Four SqCC/Y1 cell lines were seeded in EpiLife media on 6-well culture plates at the density of 1.5×10^5 cells/well just before the recording. Nine regions in each well were photographed at intervals of 10 min for the first 3 h and at 15 min intervals continuing for 48 h. For each selected region 198 images were acquired. Video files were generated from the images; a total of nine video files were obtained for each cell line (total 36 videos). Finally, 100 frames in each video were selected for analysis, while images with rounded cell shape and overgrown cultures were excluded. Thereby 900 frames for each of the four cell lines were included in the cell tracking analysis. MetaMorph (Molecular Devices Corp.) software was used for cell tracking. X and Y coordinate values for 16 cells/video/region at every frame ($n = 100$) were recorded to represent random cell migration, thereby 144 cells in each cell line were analyzed. Generated 57600 coordinates were used for later retrieval and analysis using Fiji software (NIH, Bethesda). Chemotaxis and Migration Tool in the Fiji plugin was used for analysis. ‘Plot graph’ was used to plot cell trajectories/ paths and the ‘diagram feature’ tool was selected to display a rose diagram to observe directionality between different cell lines. Velocity, accumulated and Euclidean distance were measured to quantify differences. ‘Accumulated distance’ for each track/cell that can be defined as the total distance covered or migrated within a trajectory (Fig 9). The ‘Euclidean distance’ is the measure of the mean distance between the end point and origin of each track/cell (Fig 9).

4.6 Myoma discs and Myogel (II, III)

In order to study 3D OSCC *in vitro*, our research group in Oulu has developed a human myoma organotypic model (myoma disc) using human uterine leiomyoma tissue (Nurmenniemi et al., 2009). Myoma discs contain several extracellular matrix and basement membrane (BM) proteins, as well as non-vital fibroblasts and inflammatory cells. Therefore, this model mimics the native human TME better

than the commonly used rat tail type I collagen, sometimes mixed within mouse EHS-tumor matrix (Matrigel[®]). Our group has also developed a novel solution from the myoma disc protein extracts, Myogel, which was prepared according to the Matrigel[®] preparation method. Briefly, frozen myoma tissue is ground to a powder and suspended in sodium chloride (NaCl) buffer. After centrifugation, the pellet is homogenized in the same NaCl buffer and the protein concentration in each preparation is measured (II).

A. 2D culture



B. 3D culture

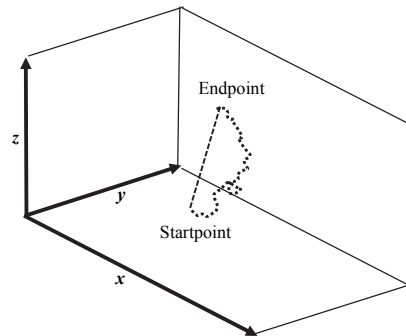


Fig. 9. Accumulated and Euclidean distance trajectories in 2D (A) and 3D (B) cultures. Accumulated distance for each track/cell that can be defined as the total distance covered within a trajectory. Euclidean distance is the distance between the end point and origin of each track/cell.

4.6.1 Rheology of Myogel (III)

The rheology of Myogel, Matrigel[®] (BD Matrigel Matrix, BD Biosciences) and their mixtures with rat tail type I collagen (BD Biosciences) Myogel-collagen, and Matrigel[®]-collagen were studied following a protocol previously published with some modification (Van Goethem, Poincloux, Gauffre, Maridonneau-Parini, & Le Cabec, 2010). Matrix samples were prepared, mixed and diluted with serum free 1:1 DMEM/F-12 medium (Life Technologies) at 4°C prior to the experiment. Final concentrations of matrices were Myogel (2.4 mg/ml), Matrigel[®] (2.4 mg/ml), Myogel-collagen mixture (2.4 mg/ml, 1 mg/ml), and Matrigel[®]-collagen mixture

(2.4 mg/ml, 1 mg/ml). Matrix responses to oscillatory shear were measured using a rheometer (Discovery HR-1, TA Instruments) equipped with a cone (40 mm diameter; 2° angle) and plate geometry. Diluted matrix gels (0.65-0.7 ml) were then placed on the center of the lower plate. The cone was lowered to the measuring gap and the plate was heated to 37°C. Matrix gels were left undisturbed in a humid atmosphere for 30 minutes for gel polymerization. After 30 minutes, the storage modulus (G'), loss modulus (G'') and complex viscosity (η^*) were measured with two different methods. A logarithmic strain sweep from 0.1 to 300% was performed, using an angular frequency of 10 rad/s, in order to evaluate the linear viscoelastic region of the gels. A linear frequency sweep from 0.1 to 0.55 Hz, using 1% strain, was performed at the linear viscoelastic region to observe the gels behavior under different angular frequencies.

4.7 Vertical migration and invasion assay (III)

The assays were performed according to published protocols described previously (Brown et al., 2014; Salo et al., 2015). They were completed with 24-well Transwell® nylon filter membrane inserts (Corning Inc.). SqCC/Y1 cell lines (1×10^5) in serum-free 100 μ l 1:1 DMEM/F-12 medium (Life Technologies) plus 1% BSA were placed on the upper compartment of the insert. 0.5 ml keratinocyte growth medium (KGM) was placed in the bottom well. Then they were incubated at 37°C in a 5% CO₂ humidified atmosphere for 24-96 h. After incubation, the media from the upper compartment was gently removed and the filters were fixed with 4% formalin for at least 1 h in RT. The remaining cells attached on the upper surface of the nylon filter membrane were carefully wiped and removed with a cotton swab. Cells on the lower surface of the membrane were stained with a Toluidine blue solution (filtered 1 % Toluidine Blue + 1 % disodium tetraborate in ddH₂O) for 10 min and later lysed with 1% SDS. The relative cell number was measured by absorbance at 650 nm.

For Transwell® invasion assays, Myogel was mixed with low-melting agarose (Myogel-LMA) for better polymerization. Myogel was diluted in serum-free medium with a final protein concentration of 2.4 mg/ml. Later 0.2% LMA was added to make Myogel-LMA gel mixture. Matrigel® was diluted in serum-free culture medium with a similar final concentration of 2.4 mg/ml. 50 μ l of the Myogel-LMA and Matrigel® were gently added at the center of the upper compartment of the insert. Incubation at RT for 30 min allowed them to polymerize.

Then the cells were seeded on top of the gels and the plates were kept for 96 h in an incubator at 37°C.

4.8 Hanging drop spheroid cultures (II)

The spheroids were formed according to the published protocol by (Del Duca, Werbowetski, & Del Maestro, 2004). HSC-3 (H2B-GFP) cells were cultured to confluency, trypsinized, washed in phosphate-buffered saline (PBS), and resuspended in DMEM/F12 medium with 10% FBS. 20 µl drops of the cell suspension were placed onto the lids of 10 cm dishes, which were inverted over dishes containing 10 ml of PBS. Hanging drop cultures were incubated for 72 h, the resulting cellular aggregates were harvested by embedding in two different conditions low-melting agarose (LMA) and Myogel-LMA (2.4 mg/ml Myogel mixed with 0.2% LMA) using a pipette, and introduced into a well of a 48 well plate. Pictures of the spheroids were taken with an EVOS inverted microscope at 0 h, 24 h, 48 h and 72 h after embedding. ImageJ software was used to measure the spheroid area and the results were calculated as a percentage of the area of the implanted spheroid.

4.9 Adhesion assay (II, III)

A cell adhesion assay was conducted to determine how many cells bind to Myogel compared to Matrigel®. The adhesion assay was performed according to a published protocol (Laaksonen et al., 2008). 96 well plates were coated for 24 hours with 100 µl of bovine serum albumin (BSA; 10 µg/ml, Sigma), fibronectin (FN; 10 µg/ml, Sigma), Matrigel® (0.62 mg/ml) and Myogel (0.62 mg/ml) diluted in PBS. The next day the excess liquids were removed, and the plates were incubated with 100 µl/well of 0.1% BSA for 2 h and washed with PBS. 6000 SqCC/Y1 cells in 100 µl EpiLife medium were added to each well and the plates were incubated at 37 °C in a 5% CO₂ humidified atmosphere for 2 h. The non-adherent cells were rinsed off, and the remaining cells were fixed with 10% trichloroacetic acid (TCA); they were later stained with crystal violet and quantified using an ELISA reader at 550 nm.

4.10 Immunofluorescence (IMF) in coated coverslips (III)

The studies were performed to examine the role of ECM in the Dsg3 expression in SqCC/Y1 cell lines. Coverslips were coated overnight with EpiLife medium, 0.62 mg/ml Matrigel[®], or 0.62 mg/ml Myogel diluted in EpiLife medium before cell seeding. The next day the excess liquids were removed and 6000 SqCC/Y1 cells in 100 μ l EpiLife medium were added to each well and the plates were incubated overnight at 37 °C in a 5% CO₂ humidified atmosphere. The next day, IMF procedure was carried out according to published protocol (Moftah et al., 2016). Stable expression of Dsg3 and its truncated mutants were visualized with the mouse mAb 5H10 in conjunction with anti-mouse IgG conjugated with Alexa Fluor 568, as described previously (Moftah et al., 2016). In addition, expression and distribution of E-cadherin and F-actin were also analyzed by fluorescent staining with the monoclonal antibody against E-cadherin HECD-1 and A488 conjugated phalloidin. Images were acquired on Leica DMI4000 B epifluorescent microscope. Image analysis was performed using ImageJ.

4.11 3D hanging drop method (II)

The collagen gel was prepared as described by the manufacturer's protocol (BD Biosciences) to make the final concentration of the collagen to be 1.7 mg/ml. The Matrigel[®]-collagen (1.5 mg/ml, 1.5 mg/ml) and Myogel-collagen (4.3 mg/ml, 1.5 mg/ml,) mixture was prepared in the same manner. 7×10^4 HSC-3 (H2B-GFP) cells were dissolved in 10 μ l DMEM/F12 medium (Life Technologies) supplemented with 2% FBS (Life Technologies), then 50 μ l matrix mixture was added. 20 μ l of cell suspension in each matrix gently pipetted on the four compartment plate. Culture plate was flipped around after 5 min of incubation in culturing condition and hanged for 3 h in the humidified chamber in culturing condition before time-lapse microscopy.

4.12 3D sandwich culture (III)

Transduced SqCC/Y1 cell lines containing nuclear lentiviral particles were embedded between two layers of polymerized 3D TME gel matrix mixtures prepared according to a published protocol with modifications (Akerfelt et al., 2015). This 3D culture method can be performed in μ -Plate Angiogenesis 96 Well (Ibidi) featuring a well-in-a-well geometry consisting of two compartments

(smaller & larger), the smaller compartment is in the bottom of the larger one. Rat tail type I collagen (2.4 mg/ ml), Matrigel[®] (2.4 mg/ ml), Matrigel[®]-collagen and Myogel-collagen mixtures were used as ECM. In the Matrigel[®]-collagen and Myogel-collagen mixtures the final protein concentrations were for Myogel/Matrigel[®] (2.4 mg/ ml) and for Collagen (1 mg/ ml). The smaller (bottom) compartment was first filled with 10 μ l of matrix mixture. The plates were kept gently in an incubator at 37 °C for 30 min to 1 h for polymerization and were then centrifuged for 20 mins at 200 \times g in RT. Cell suspensions (1500 cells/well) were embedded in 20 μ l ECM mixture and placed on top of the polymerized bottom gel. Then the plates were centrifuged for 10 mins at 100 \times g and the upper gel with cells embedded was allowed to polymerize by overnight incubation at 37 °C in a 5 % CO₂ humidified atmosphere. Sterile PBS was added into the outer wells and rim for better humidity control. 20 μ l KGM medium containing 2% heat inactivated fetal bovine serum (FBS; Life Technologies) was added on top gently prior to 24 h time-lapse microscopy.

In co-cultures, transduced Ct-H2B and two mutants (Δ 238-H2B & Δ 560-H2B) were used alongside CAF-GFPs and NOFs. The ratio of SqCC/Y1 cells to fibroblasts (2:1) was optimized for standard stromal interaction formation. 1000 cancer cells were gently mixed with 500 CAF-GFPs or NOFs separately, and later the total co-culture cell suspensions (1500 cells/well) were embedded in Myogel-collagen (2.4 mg/ ml, 1 mg/ ml).

4.13 AK23 antibody treatment against Dsg3 (III)

Mouse monoclonal antibody acantholytic keratinocyte AK23 (MBL, Japan), which binds to the first extracellular domain of Dsg3 was used (Tsunoda et al., 2003). We aimed to test the inhibitory activity of AK23 mouse monoclonal antibodies against Dsg3 on SqCC/Y1 cell invasion using the 3D sandwich culture assay as explained in (Akerfelt et al., 2015). AK23 and mouse IgG1 isotype control were mixed gently in the Myogel-collagen (2.4 mg/ ml, 1 mg/ ml) mixture with 1 μ g/ml final concentration before cell embedding as suggested in the manufacturer's instructions. All four transduced fluorescent-labeled cells were then embedded in a Myogel-collagen matrix containing AK23 and IgG1. Later the cells were treated with either IgG1 isotype control or AK23, at 1 μ g/ml concentration in KGM (Gibco) medium containing 2% FBS (Life Technologies).

4.14 3D image acquisition and time-lapse microscopy

4.14.1 *Spinning disc confocal microscopy (II)*

In 3D hanging drops, images of transduced HSC-3 cells were taken with spinning disc confocal microscope (Zeiss, Germany) using Zeiss Cell 21 with EC Plan-Neoflaur 40x/0.75 M27 objective, and two channels (mCherry and GFP). Images were taken in every 15 minutes with 19.8 μm Z spacing with Hamamatsu Camera#2 controlled by Zen Blue 2012 software (Zeiss, Germany) for 22 hours.

4.14.2 *Epifluorescence microscopy and deconvolution (III)*

To visualize the transduced SqCC/Y1 cell lines and CAFs in 3D sandwich cultures at 37 °C in 5% CO₂ humidified atmosphere, CellSens system (Olympus, Japan) with its top stage incubator was utilized. Images were taken with CPlanFLN PhC 10x/0.30, UPlanFLN 20x/0.50 objectives (Olympus, Japan) for TxRed and GFP channels. Images were taken every 30 min with 7.9 μm Z spacing with Olympus XM10 CCD controlled by cellSens Dimension for 18–24 h. 3D image stacks were processed with Huygens Professional (Scientific Volume Imaging, the Netherlands) deconvolution wizard using initial parameters before quantitative analysis.

4.15 Myoma disc assay (III)

Organotypic myoma invasion experiments were done according to the published myoma model protocols (Nurmenniemi et al., 2009; Teppo et al., 2013). Briefly, myoma tissues were processed, cut to 5 mm slices and then into discs with an 8-mm biopsy punch (Kai Industries Co., Japan). Before the experiments, myoma discs were equilibrated and rinsed by gentle rotation in KGM containing 10% FBS at 4°C for 48 h. Rinsed discs were carefully placed in the 6.5 mm diameter Transwell® inserts (Corning, NY, USA) and 7×10^5 SqCC/Y1 cells suspended in 50 μl of serum free 1:1 DMEM/F-12 medium plus 1% BSA were added on top. 0.5 ml KGM containing 10% FBS was added in the wells, and the cells were allowed to attach overnight in an incubator at 37°C in a 5 % CO₂ humidified atmosphere. On the following day, myoma discs with cells attached on top were placed onto nylon discs on curved steel grids in 12 well plates with 1 ml of KGM containing 10% FBS in each well. The cells were cultured for 14 days. The medium was changed in the bottom well on days 4, 7, 10, and 13. On the 14th day, the cultures were fixed

with 4% formalin for 24 h at RT. The results were analyzed after histological procedures. The invasion patterns of four SqCC/Y1 cell lines were quantified after immunohistochemical pancytokeratin AE1/AE3 (Dako) staining to identify SqCC/Y1 cells. Sections were digitally recorded at $\times 100$ magnification with a DMRB photo microscope connected to a DFC 480 camera using QWin V3 software (Leica Microsystems). The areas of stained non-invading and invading cells were measured, excluding the nonuniform invasion in the edges of the myoma. Invasion area and depth were measured with ImageJ.

4.16 Statistical analysis (I, II, III)

Statistical evaluation was performed using student t-test of Microsoft Excel (Office 2013; Microsoft Corp, Redmond, WA) and ANOVA of IBM SPSS 23.0 software for Windows (SPSS Inc., Chicago, IL, USA). Statistical tests applied for data analysis are indicated in the figure legends. We considered a P-value of <0.05 to be statistically significant and are indicated with asterisks. Graphic indications of calculated p-values are * $p < 0.05$ and > 0.01 , ** $p < 0.01$ and > 0.001 ; *** $p < 0.001$.

4.17 Ethical considerations (II, III)

The human myoma studies were approved by the Ethical Committee of the Oulu University Hospital, Finland (8/2006, 26/2006, 4/2014 and 35/2014).

5 Results

5.1 Detecting C-terminally truncated mutants

We earlier reported the overexpressed FL (Tsang et al., 2010). The expression of the C-terminus of FL and truncated Dsg3 proteins were measured by immunofluorescence using the rabbit anti-Myc tag antibody, which detects the Myc tag epitope. Strong expression was detected in FL cells, and restricted, cytoplasmic staining in mutant cell lines $\Delta 238$ and $\Delta 560$. These results indicated the normal function of exogenous Dsg3 in FL, and the lack of a transmembrane domain in the two truncated proteins (Fig 10).

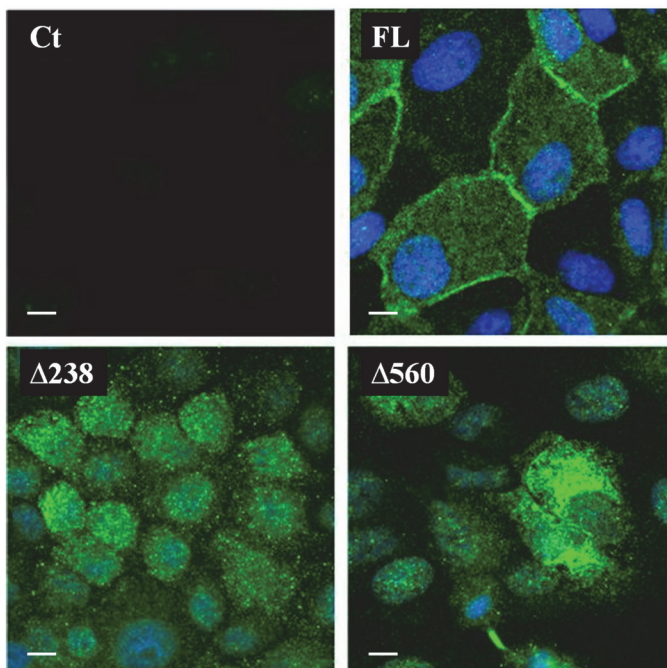


Fig. 10. Fluorescent microscopic images of SqCC/Y1 cell lines with transduction of Ct, full length FL and two Dsg3 truncated mutants, $\Delta 238$, and $\Delta 560$. Cells were stained with the rabbit Myc tag Ab and A488 conjugated rabbit IgG. In contrast to FL cells, where Dsg3 was in the cell membrane, in both mutants the Myc was located in the cytoplasm. Scale bar, 10 μm .

Western blots with anti-Myc tag antibody of total lysates from SqCC/Y1 cell lines confirmed that the molecular weights were similar to the calculated ones;

approximately 200 kDa for Ct, 130 kDa for FL, 40 kDa for $\Delta 238$, and 80 kDa for $\Delta 560$. For $\Delta 238$ the molecular weight of Dsg3 was slightly larger than the calculated 35 kDa (Fig 1B in I).

5.2 Expression of Dsg3 truncated proteins caused compromised cell-cell adhesions

Our previous study has shown that Dsg3 depletion in epithelial cells causes cell cohesion, which results in an enhanced fragmentation of epithelial sheets, as assessed by the dispase dissociation assay (Mannan et al., 2011). Tsang et al. (2010) suggested that Dsg3 overexpression causes disrupted junctional assembly. Later they supported this finding by showing that Dsg3 acts outside of the DSMs, combined with E-cadherin and by activating Src signaling (Tsang et al., 2012).

To determine if cell lines which express truncated Dsg3 proteins exhibit the same phenotypes in cell-cell adhesions we performed a similar dispase dissociation assay as described above. Fragmentation of epithelial sheets was induced by mechanical stress through pipetting the samples (Fig 1C, after in I). The results showed a significant increase of fragments in all mutant cell lines compared to Ct or FL cells (Bar chart, Fig 1C in I). This suggests that the expression of Dsg3 truncated proteins causes weakening of cell-cell adhesions and disruption of epithelial integrity. No significant difference was observed between Ct and FL epithelial sheets, and their integrity was almost intact. During the dispase treatment, mutant cell lines formed compromised cell-cell adhesions in the monolayer.

To determine the Dsg3 distribution in cell-cell attachments in Ct, FL, and $\Delta 238$ cell lines, IMF experiments were carried out using mouse anti-Dsg3, and rabbit anti-Myc tag Abs. Strong membrane staining was observed with mouse anti-Dsg3 in all cell lines (Green staining, Fig 2A in I) which indicates membrane localization of both native and exogenous overexpressed Dsg3. Nevertheless, mutant $\Delta 238$ cell-cell junctions presented disrupted Dsg3 distribution (Fig 2A in I). Compromised cell-cell adhesion in mutant cells indicates defected junctional protein organization. Collectively, these results suggest that, similar to Dsg3 depletion, the expression of Dsg3 C-terminally truncated proteins reduces the cell cohesion and disrupts structural integrity in epithelial sheets.

We also studied the adhesion of Ct, FL, $\Delta 238$, and $\Delta 560$ cell lines cultured on top of BSA, FN, Matrigel[®], and Myogel. The adhesion of Ct and FL on top of Myogel coated wells was lower than on Matrigel[®] ($p < 0.001$ and $p = 0.04$, respectively, Supplementary Fig S3 in III). By contrast, $\Delta 560$ cells adhered more

on Myogel ($p = 0.04$) than on Matrigel[®], whereas on every substrate, $\Delta 238$ mutants adhered almost similarly. Compared to Ct, both mutants, $\Delta 238$ ($p < 0.01$) and $\Delta 560$ ($p < 0.001$) adhered less on Matrigel[®] (Supplementary Fig S3 in III). However compared to Ct on top of Myogel, FL and both mutants did not exhibit significantly different adhesion (Supplementary Fig S3 in III).

5.3 Dsg3 affects both horizontal and vertical migration in buccal carcinoma cells

To determine the role of Dsg3 in horizontal cell migration, Ct, FL, $\Delta 238$, and $\Delta 560$ cell lines were cultured in the IncuCyte[™] live cell imaging system. After tracking the cells, we quantified 2D migration pattern, trajectory, and directionality. We also analyzed the mean velocity, accumulated and Euclidean distances.

After importing the selected datasets, the trajectory of each cell line was plotted (Fig 1B in III). The majority of Ct cells moved similarly, almost half of the FL cells migrated further than Ct and they turned differently. Compared to Ct, $\Delta 238$ cells migrated irregularly and in restricted patterns. $\Delta 560$ cells migrated far but most of them returned near to the original point (Fig 1B in III). The directionality of cell migration in four cell lines are presented by a ‘rose diagram’. FL and mutants migrated in more limited directions than Ct cells (Fig 1C in III). Compared to the Ct, mean migration velocities of FL ($p < 0.001$) and two mutants ($p < 0.001$) were higher (Fig 1D in III). FL ($p < 0.001$) and the two mutants ($p < 0.001$) had greater accumulated distances than Ct (Fig 1E in III). Increased Euclidean distances were measured only in FL ($p < 0.001$) and $\Delta 238$ ($p < 0.001$) compared to Ct (Fig 1F in III).

For vertical migration analyses, we used Transwell migration assays. Compared with Ct, after 72 h incubation the cell lines differed in their migration speed (Fig 2A in III); only the mutant $\Delta 238$ migrated faster ($p < 0.001$) than other three cell lines. At 96 h, more FL ($p < 0.001$), $\Delta 238$ ($p < 0.001$) and $\Delta 560$ ($p < 0.01$) cell lines than Ct had passed through the membrane. The migration of the Mutant $\Delta 238$ was significantly faster ($p < 0.001$) than FL and the other mutant $\Delta 560$ cell lines (Fig 2A in III).

5.4 Myogel is a novel matrix for studying carcinoma cell invasion

Organotypic invasion assays in this study were mainly based on the application of human uterine leiomyoma tissue derived Myogel. In Myogel, one-third of the total

proteins were the same as in Matrigel[®]. Mass spectrometry results on Myogel identified 765 proteins including major ECM proteins, such as nine laminin chains, type IV collagen, epidermal growth factor (EGF), heparan sulfate proteoglycans and nidogen 1, and 2 (Supplementary Table S1 in II). Compared to Matrigel[®], the pH of Myogel is neutral and more stable in cell culture conditions. Myogel combined with low-melting agarose (LMA), or type 1 collagen, can be used in a gelatinous form to mimic the TMEM for cancer cells.

To explore different rheological parameters of Myogel compared with Matrigel[®], Matrigel[®]-collagen, and Myogel-collagen, we tested stiffness and viscosity. In various frequency ranges, Myogel was softer and less viscous than Matrigel[®] (Supplementary Fig S2A-D in III). In the strain sweep technique, Myogel-collagen was compared with Myogel, Matrigel[®] and Matrigel[®]-collagen (Supplementary Fig S2C-D in III). Myogel-collagen was stiffer and more viscous than Myogel, but less viscous than Matrigel[®], and Matrigel[®]-collagen. Myogel is less stiff and viscous than Myogel-collagen & Matrigel[®] (Supplementary Fig S2C-D in III). However, Matrigel[®]-collagen were stiffer and viscous than all other matrices (Supplementary Fig S2C-D in III).

Myogel is a helpful tool to study carcinoma cell behavior, adhesion, migration and invasion. Tongue HSC-3 cells adhered significantly more to Matrigel[®] coated wells than to Myogel coated ones (Fig 1 in II). In scratch assays, carcinoma cells migrated faster in Myogel coated wells than in Matrigel[®] (Fig 3A-B in II), and similarly, in transwells, HSC-3 cells invaded faster through Myogel than Matrigel[®] (Fig 4 in II).

5.5 Buccal SCC cells invade faster in leiomyoma derived matrices

We investigated how variations of Dsg3 structures differentiates the invasiveness of four buccal SqCC/Y1 cell lines (Ct, FL, Δ 238, and Δ 560), using Transwell invasion assays and organotypic myoma discs.

In Transwell invasion assays, Ct ($p < 0.01$), Δ 238 ($p < 0.001$) and Δ 560 ($p < 0.05$) cell lines invaded significantly faster through Myogel-LMA compared to the Matrigel[®] coated wells (Fig 2B in III). Through Myogel-LMA coating, FL ($p < 0.01$) and mutant Δ 238 ($p < 0.001$) cells invaded faster (Fig 2B in III) than the controls. Between the two mutants, Δ 238 ($p < 0.01$) cells invaded faster than Δ 560 cells through Myogel-LMA coating. However, through Matrigel[®] compared to the Ct, only the FL ($p < 0.01$) cells exhibited higher invasion (Fig 2B in III).

In myoma disc assays, $\Delta 238$ mutants invaded more than Ct ($p < 0.01$), FL ($p < 0.01$) and other mutant $\Delta 560$ ($p < 0.05$) cell lines. Mutant $\Delta 238$ invaded deeper through the myoma discs compared to Ct ($p < 0.001$), FL ($p < 0.001$) and mutant $\Delta 560$ ($p < 0.01$) cell lines (Fig 6A-C in III). A brief summary of all findings is presented in Table 1 in (III).

5.6 OSCC cell invasion depends on the microenvironment

To study how the microenvironment affects OSCC cell invasion, tongue HSC-3 cells were embedded within 3D hanging drop cultures and four buccal SqCC/Y1 cell lines were embedded within the 3D sandwich using different TME matrices for 18-20 h.

5.6.1 Tongue SCC cell invasion in 3D hanging drops

We optimized this technique to observe the cell behavior in different 3D matrices (II). In hanging drops, HSC-3 cells moved similarly within collagen, Myogel-collagen, and Matrigel[®]-collagen. However, tongue carcinoma cells moved faster in Myogel-collagen than in both collagen and Matrigel[®]-collagen in the 3D hanging drop cultures (Supplementary Fig S2 in II).

5.6.2 Buccal SCC cell invasion in 3D sandwich

We used this method to quantitatively analyze speed, accumulated and Euclidean distances of SqCC/Y1 cell lines embedded within various TME matrices (collagen, Matrigel[®], Myogel-collagen, and Matrigel[®]-collagen). Both ΔC -H2B mutants invaded faster than Ct and FL cell lines within Matrigel[®] and Matrigel[®]-collagen (Fig 3A in III). Within collagen and Myogel-collagen, FL and the truncated cell lines were faster than the Ct (Fig 3A in III). However, ΔC -H2B mutants moved faster than FL-H2B in all matrices. The accumulated distances within collagen were higher in FL and ΔC -H2B mutants than in Ct (Fig 3B in III). Compared with Ct, in Matrigel[®] and Matrigel[®]-collagen, both mutants had increased accumulated distances (Fig 3B in III). In Myogel-collagen, three cell lines had higher accumulated distances compared to Ct (Fig 3B in III). Both mutants had higher Euclidean distances in collagen, Matrigel[®], and Matrigel[®]-collagen (Fig 3C in III), and within Myogel-collagen, FL-H2B and $\Delta 238$ -H2B had increased Euclidean distances compared to Ct cells (Fig 3C in III).

5.7 OSCC cells interact with fibroblasts in 3D sandwich

We investigated how buccal SqCC/Y1 cell lines behave while interacting with CAFs or normal oral fibroblasts (NOF) within Myogel-collagen matrix using 3D sandwich technique. In monocultures, both mutants had higher invasion speeds compared to Ct (Fig 4A in III). In co-cultures with CAFs, $\Delta 238$ cells invaded faster than control or $\Delta 560$ cells (Fig 4B in III). In co-cultures with NOFs, Ct moved faster than both mutants (Fig 4C in III).

5.8 Antibody treatment alters the invasion pattern in buccal SCC cells in 3D sandwich

We experimented to observe whether the anti-Dsg3 antibody inhibits carcinoma cell invasion by targeting the adhesion site on the N-terminus of Dsg3. We used the monoclonal antibody AK23, which binds to the first extracellular domain EC1 of Dsg3 (III). We tested whether the AK23 antibody is able to inhibit Dsg3 action on the invasion velocity of SqCC/Y1-H2B cell lines within Myogel-collagen matrix using 3D sandwich. Overexpressed FL-H2B cells treated with AK23 moved slower compared with an IgG1 isotype control (Fig 5B in III). The AK23 antibody did not affect the invasion speed of other cell lines (Fig 5A, C-D in III).

6 Discussion

6.1 Dsg3 promotes migration and invasion of OSCC cell lines

Dsg3 was first recognized as a PV antigen while searching PV autoantibody targets (Wan, 2018). However, the explicit role of Dsg3 in cancer initiation and progression is still unknown (Brown & Wan, 2015). The traditional view of the Dsg3 function is that it acts solely as a structural adhesive protein in DSMs. Tsang et al. demonstrated that Dsg3 overexpression in epithelial cell lines caused dysfunction of a range of cadherins in both DSMs and AJs (Tsang et al., 2010). In support of this observation, they later showed that a small pool of Dsg3 functions outside of the DSMs, being associated with E-cadherin and activating Src signaling within the E-cadherin complex (Tsang et al., 2012). We previously reported that Dsg3 promotes migration and invasion in epidermoid carcinoma and FL cells by activation of several signaling pathways, which have a negative impact on E-cadherin adhesion and the actin cytoskeleton. We measured their invasion in Matrigel[®] and Matrigel[®]-collagen organotypic cultures (Brown et al., 2014; Tsang et al., 2010). We also showed then that Dsg3 promotes cancer cell migration and invasion by regulating activator protein 1 (AP-1), and protein kinase C (PKC) in OSCC (Brown et al., 2014). Moreover, RNAi and shRNA knockdown of Dsg3 inhibits migration of several OSCC cell lines (Chen et al., 2007; Chen et al., 2013). However, a recent study reported the opposite effect; with overexpression of Dsg3, HaCaT cells migrate slowly and siRNA silencing of Dsg3 accelerates the cell migration in a 2D culture setting (Rotzer et al., 2015). The logic for this difference is unclear, but it could well be due to the different types of keratinocyte cell lines.

We earlier showed that the expression of ΔC mutants in SqCC/Y1 resulted in a defect in DSMs and cell-to-cell adhesion (I), which likely arose from the changes in cell migratory behavior, as observed in this study. Indeed, we demonstrated the reduced expression and distribution of both Dsg3 and E-cadherin at the cell periphery in mutant cells. Based on these findings, we hypothesized that disruption of the cell to cell adhesion in Dsg3 mutant cells may affect cell migration and invasion (I). Our findings will report the Dsg3 mutants in cancer cell migration and invasion, compared it with FL cells which are known to have enhanced cell motility (III).

We have reported that reduced surface expression of plakoglobin (Pg) and p120-catenins along with Dsg3 in mutants, suggesting a defect in surface junction

protein assembly (I), Pg and p120 are essential for DSM junction formation. The C truncated mutants also exhibited reduced Rab proteins, which is crucial for intracellular signaling, and membrane trafficking (I). In 2D culture, FL cells migrated faster than Ct; which supports our previous findings (Brown et al., 2014; Tsang et al., 2010). Additionally, we quantified the cell migration in two ΔC mutants whose migration behavior had not been studied before, and we found the mutants also presented similar increased migration activity. Also, we investigated the role of Dsg3 in SqCC/Y1 cell invasion by using Myogel and the solid myoma discs (Nurmenniemi et al., 2009) compared with collagen, and Matrigel[®]. In Transwells, FL and two ΔC mutants invaded faster than the Ct (III), and the results are consistent with our previous findings (Brown et al., 2014). In our 3D sandwich, only the ΔC mutants invaded significantly faster than Ct, and CAFs induced invasion of the shorter $\Delta 238$ mutant (III). We also used solid myoma discs to study invasion, where both mutants were more invasive (III). Briefly, cells expressing Dsg3 ΔC mutants exhibited enhanced migration and invasion, suggesting that loss of Dsg3 action promotes cell motility in the human TME matrix. This is likely caused by defects in E-cadherin trafficking, cell-to-cell adhesion, and junctional assembly in cells expressing Dsg3 ΔC mutants.

There was no clinical evidence of Dsg3 truncated mutations in human diseases until most recently, a homozygous nonsense mutation in the Dsg3 gene has been identified in human for the first time, causing recurrent blisters, and erosion in the oral mucosa of a one-year-old female baby (Kim et al., 2018). Therefore, it is of great value to learn the biological consequences of these Dsg3 truncated mutants in a wide range of cellular processes that likely contribute to the pathogenesis of associated diseases.

6.2 Leiomyoma derived TME matrices affect OSCC cell invasion

The tumor microenvironment (TME) plays a leading role in cancer spreading. Its components control cancer progression. The interaction between cancer cells and TME modulates structural and functional changes of solid tumors (Salo et al., 2014; Teppo et al., 2013). Commonly used commercial models to study cancer cell invasion are type I collagen and Matrigel[®], in which the latter is a basement membrane (BM) extract (Kleinman et al., 1986). Naturally, BM separates the body surface from the underlying connective tissue and contains basal lamina, and underlying layer of reticular connective tissue (Paulsson, 1992). Both immunologically and chemically, the contents of Matrigel[®] matches the BMs

(Engbring & Kleinman, 2003). Matrigel[®] is commonly used *in vitro* to mimic BMs, but its tumor-derived matrix does not consist of all the BM components present *in vivo*. BMs act as scaffolds to support tissue structure and also play a role in cellular function (LeBleu, Macdonald, & Kalluri, 2007). It also acts as a mechanical barrier, while discouraging cancer cells from invading the adjacent tissues; prevent endothelial tube formation, and tumor growth (Tanjore & Kalluri, 2006). One study showed Matrigel[®] inhibited benign prostatic hyperplasia cell invasion (Albini et al., 1987). However, Matrigel[®] does not completely simulate the actual human TME because of its rodent origin (Jaganathan et al., 2014; Sundquist et al., 2016). Therefore, we introduced human uterine leiomyoma tissue based myoma discs (Nurmenniemi et al., 2009) and gelatinous Myogel (II) for 3D *in vitro* invasion studies.

Nurmenniemi et al. first described the use of the myomas in 2009, and since then they are used in invasion studies with various cells in which carcinoma cells invaded the myomas more than in other matrices. They include several types of human tongue OSCC cell lines (Aikio et al., 2012; Alahuhta et al., 2015; Al-Samadi et al., 2017; Astrom et al., 2017; Bitu et al., 2013; Dayan et al., 2012; Nurmenniemi et al., 2010; Pirila et al., 2015; Salo et al., 2013; Sundquist et al., 2016; Teppo et al., 2013; Vered et al., 2015; Vilen et al., 2012), human mucoepidermoid carcinoma cells (Korvala et al., 2014), lung adenocarcinoma and SCC cells (Merikallio et al., 2012), malignant melanoma UT-MUC-1, and ductal breast adenocarcinoma MDA-MB-231 cells (Sundquist et al., 2016). Among the many studies included stromal fibroblasts, such as CAFs (Dayan et al., 2012; Sundquist et al., 2016), NOFs (Sundquist et al., 2016), human gingival fibroblasts (GFs) (Dayan et al., 2012; Vered et al., 2015), CaDEC12 cells (Vered et al., 2015), and immune cells like macrophages (Pirila et al., 2015). In our current study with oral buccal SCC cell lines, the ΔC mutants invaded more through myoma discs (III).

Myogel includes major ECM proteins similar to myoma discs (II). Both Myogel and Matrigel[®] contains similar proteins such as laminin, type IV collagen, heparan sulfate proteoglycans, nidogen and EGF. Although, 34% (259 out of the 765) of the total identified matrix proteins are present in both Myogel and Matrigel[®] (II), myoma tissue contains also additional factors required for carcinoma cell invasion, such as tenascin-C (TNC) (Sundquist et al., 2016), active forms of MMP-2 (Nurmenniemi et al., 2009), and LOX-1 (Teppo et al., 2013). Furthermore, multiple soluble growth factors, their receptors, and other binding proteins identified in myoma discs, and many of them, such as TGF- β 1 and 2, HGF, and FGF2, engage in carcinoma cell movement (Sundquist et al., 2016; Teppo et al.,

2013). These microenvironmental features are crucial to induce carcinoma invasion. We even tested to find out whether non-cancerous tissues, such as the human heart and porcine tongue induce carcinoma cell invasion. Compared to the myomas, human OTSCC cells invaded decidedly less in human heart tissue, whereas they did not invade in porcine tongue (Sundquist et al., 2016). However, solid myoma discs are more realistic for 3D carcinoma cell invasion. In addition to collagen fiber assembly and other ECM molecules, they also contain non-vital, inflammatory, endothelial cells, and vessel structures, all of which are necessary for tumor growth and invasion (Nurmenniemi et al., 2009). As a solid tumor mass, leiomyoma derived matrices (Myoma discs and Myogel) are ideal for several cancer cell line experiments *in vitro*. Currently, other human ECM matrices used to study behaviors of cancer cell lines are derived either from normal human tissues (such as skeletal muscle, amnion membrane, and placenta) or are from *in vitro* cell cultures [MaxGel™ Human ECM (Sigma), AlphaMAX3D (Neuromics)]. The benefit of Myogel is that is not a mimic of any normal tissue (including mucosa) structure but is made by neoplastic cells within a tumor (II).

We demonstrated that Myogel combined with low-melting agarose (LMA) or with type I collagen provides an easy-to-use gelatinous TMEM for *in vitro* invasion studies (II, III). Human oral tongue SCC cell lines (HSC-3 and SCC-9), and also melanoma cell lines (SK-Mel-25 and A2058) invade faster through Myogel in comparison to type I collagen or Matrigel® (II). Previously, we showed increased invasion of FL cells compared to controls through rodent based Matrigel®, and Matrigel®-collagen matrices (Brown et al., 2014). Those results are consistent with our current findings, where FL and two ΔC mutants invaded faster through Myogel-LMA than Matrigel® coated wells in similar Transwells assays. In the sandwich assays, the cells invaded faster in Myogel-collagen than Matrigel®-collagen (III).

Here, we investigated the role of Dsg3 in the invasion with all four buccal SCC SqCC/Y1 cell lines utilizing soluble Myogel, and the solid myoma discs (III). Similar to the tongue SCC and melanoma cells, human buccal mucosa carcinoma SqCC/Y1 cells invade more in myoma tissues (III). Compared with the commercially available rodent matrices Matrigel® and rat tail type I collagen, we demonstrated once again that myoma matrices provided superior TMEM to mouse sarcoma BM extracts by promoting cell movement locomotion in the cell lines tested (II, III). As it is a BM extract, we can easily speculate that Matrigel® inhibits, while myoma derived matrices induce carcinoma cell invasion because of their human TMEM texture. The current study reestablishes our earlier finding that Myogel, alongside with myoma discs are a more physiologically relevant TMEM

for studying cancer cell movement. Therefore, based on the findings, we can explicitly say that the TME composition directly influences cancer cell invasion.

6.3 Dsg3 as a potential novel anti-cancer drug target

Monoclonal antibodies targeting EGFR are already in clinical use for OSCC. However, the clinical outcomes of these antibodies such as Cetuximab and Panitumumab are unsatisfactory (Yamamoto, Thylur, Bauschard, Schmale, & Sinha, 2016). To overcome this, researchers have been searching for new targets for monoclonal antibodies that could be useful against OSCC. As Dsg3 is overexpressed in OSCC, we hypothesized that Dsg3 could be used for targeted therapy and developed a novel method of targeting with a monoclonal antibody against it.

We studied the effectivity of the AK23 antibody, which binds to the EC1 domain of Dsg3 (Di Zenzo et al., 2012). However, this study was preliminary and the data obtained indicate that AK23 may be able to inhibit invasion of FL cells but not the mutants (III). ICDs present in FL cells may support AK23 by intercellular signaling (Fig 11). Dsg3 Δ C mutants had a negative impact on the surface expression of endogenous Dsg3, which is less likely to be bound by AK23 sufficiently.

On controls, AK23 may have less effect with a 1 μ g/ml concentration (III). A recent study conducted in Dr. Hong Wan's group in Queen Mary University has elucidated that a much higher dose (500 μ g/ml) is required to inhibit epidermoid carcinoma A431 cell migration in 2D *in vitro* studies using an IncuCyte™ system (Unpublished data). Although the effects of AK series of antibodies on cell-cell adhesion have been established, their role in inhibiting cancer is unknown.

Our preliminary study suggested that the EC domain of Dsg3 might potentially serve as a novel target for new anticancer drugs. We have to conduct *in vitro* experiments focusing on the EC domain of Dsg3 and validate whether these monoclonal antibodies (Abs) do not hamper the normal physiological cell-cell adhesion initiated by the domain. We still have to continue testing AK23 vigorously, using 2D and 3D techniques in order to eliminate the risk of disrupting EC1 domain, since there is a possibility of defected cell-cell adhesion by the monoclonal antibody treatment. We will compare with other Abs targeting Dsg3, such as Kouno et al. suppressed OSCC cell invasion *in vitro* by aiming non-pathogenic anti-Dsg3 monoclonal antibody (Px44) by fusing it with an apoptosis-inducing ligand (Kouno, Minabe, Tachikawa, & Stanley, 2017). After possible promising *in vitro* results

with human tissue-derived ECM matrices we should still proceed to *in vivo* animal models before clinical trials.

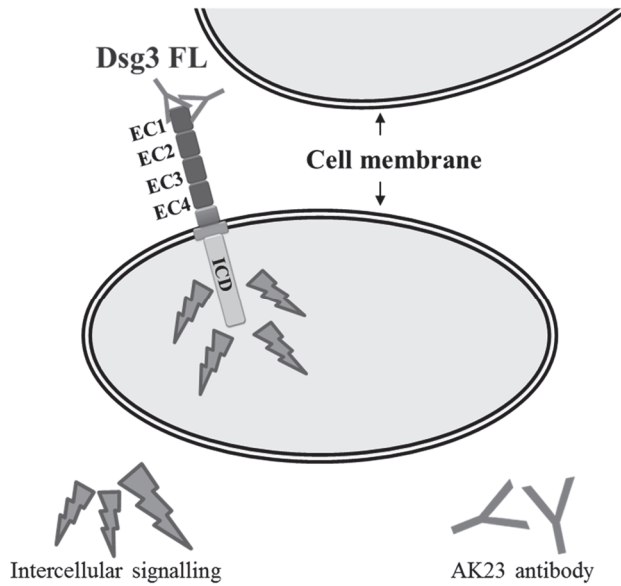


Fig. 11. Schematic diagram of monoclonal antibody (AK23) binding with first extracellular domain (EC1) of Dsg3 in FL cells.

List of references

- Abou Neel, E. A., Bozec, L., Knowles, J. C., Syed, O., Mudera, V., Day, R., & Hyun, J. K. (2013). Collagen--emerging collagen based therapies hit the patient. *Advanced Drug Delivery Reviews*, 65(4), 429-456. doi:10.1016/j.addr.2012.08.010 [doi]
- Agarwal, A. K., Sethi, A., Sareen, D., & Dhingra, S. (2011). Treatment delay in oral and oropharyngeal cancer in our population: The role of socio-economic factors and health-seeking behaviour. *Indian Journal of Otolaryngology and Head and Neck Surgery: Official Publication of the Association of Otolaryngologists of India*, 63(2), 145-150. doi:10.1007/s12070-011-0134-9 [doi]
- Aikio, M., Alahuhta, I., Nurmenniemi, S., Suojanen, J., Palovuori, R., Teppo, S., . . . Nyberg, P. (2012). Arresten, a collagen-derived angiogenesis inhibitor, suppresses invasion of squamous cell carcinoma. *PloS One*, 7(12), e51044. doi:10.1371/journal.pone.0051044 [doi]
- Akerfelt, M., Bayramoglu, N., Robinson, S., Toriseva, M., Schukov, H. P., Harma, V., . . . Nees, M. (2015). Automated tracking of tumor-stroma morphology in microtissues identifies functional targets within the tumor microenvironment for therapeutic intervention. *Oncotarget*, 6(30), 30035-30056. doi:10.18632/oncotarget.5046 [doi]
- Alahuhta, I., Aikio, M., Vayrynen, O., Nurmenniemi, S., Suojanen, J., Teppo, S., . . . Nyberg, P. (2015). Endostatin induces proliferation of oral carcinoma cells but its effect on invasion is modified by the tumor microenvironment. *Experimental Cell Research*, 336(1), 130-140. doi:10.1016/j.yexcr.2015.06.012 [doi]
- Al-Amoudi, A., Chang, J. J., Leforestier, A., McDowall, A., Salamin, L. M., Norlen, L. P., . . . Dubochet, J. (2004). Cryo-electron microscopy of vitreous sections. *The EMBO Journal*, 23(18), 3583-3588. doi:10.1038/sj.emboj.7600366 [doi]
- Alberts, B., Johnson, A., Lewis, J., Raff, M., Roberts, K., & Walter, P. (2002). *Cell junctions* Garland Science. Retrieved from <https://www.ncbi.nlm.nih.gov/books/NBK26857/>
- Albini, A., Iwamoto, Y., Kleinman, H. K., Martin, G. R., Aaronson, S. A., Kozlowski, J. M., & McEwan, R. N. (1987). A rapid in vitro assay for quantitating the invasive potential of tumor cells. *Cancer Research*, 47(12), 3239-3245.
- Allen, E., Yu, Q. C., & Fuchs, E. (1996). Mice expressing a mutant desmosomal cadherin exhibit abnormalities in desmosomes, proliferation, and epidermal differentiation. *The Journal of Cell Biology*, 133(6), 1367-1382.
- Almangush, A., Bello, I. O., Keski-Santti, H., Makinen, L. K., Kauppila, J. H., Pukkila, M., . . . Salo, T. (2014). Depth of invasion, tumor budding, and worst pattern of invasion: Prognostic indicators in early-stage oral tongue cancer. *Head & Neck*, 36(6), 811-818. doi:10.1002/hed.23380 [doi]
- Almangush, A., Coletta, R. D., Bello, I. O., Bitu, C., Keski-Santti, H., Makinen, L. K., . . . Salo, T. (2015). A simple novel prognostic model for early stage oral tongue cancer. *International Journal of Oral and Maxillofacial Surgery*, 44(2), 143-150. doi:10.1016/j.ijom.2014.10.004 [doi]

- Al-Samadi, A., Awad, S. A., Tuomainen, K., Zhao, Y., Salem, A., Parikka, M., & Salo, T. (2017). Crosstalk between tongue carcinoma cells, extracellular vesicles, and immune cells in in vitro and in vivo models. *Oncotarget*, *8*(36), 60123-60134. doi:10.18632/oncotarget.17768 [doi]
- Amagai, M., Ishii, K., Hashimoto, T., Gamou, S., Shimizu, N., & Nishikawa, T. (1995). Conformational epitopes of pemphigus antigens (Dsg1 and Dsg3) are calcium dependent and glycosylation independent. *The Journal of Investigative Dermatology*, *105*(2), 243-247. doi:S0022-202X(15)42285-7 [pii]
- Amagai, M., Klaus-Kovtun, V., & Stanley, J. R. (1991). Autoantibodies against a novel epithelial cadherin in pemphigus vulgaris, a disease of cell adhesion. *Cell*, *67*(5), 869-877. doi:0092-8674(91)90360-B [pii]
- Amagai, M., Tsunoda, K., Zillikens, D., Nagai, T., & Nishikawa, T. (1999). The clinical phenotype of pemphigus is defined by the anti-desmoglein autoantibody profile. *Journal of the American Academy of Dermatology*, *40*(2 Pt 1), 167-170. doi:S0190-9622(99)70183-0 [pii]
- Angst, B. D., Marcozzi, C., & Magee, A. I. (2001). The cadherin superfamily: Diversity in form and function. *Journal of Cell Science*, *114*(Pt 4), 629-641.
- Anguiano, M., Castilla, C., Maska, M., Ederra, C., Pelaez, R., Morales, X., . . . Ortiz-de-Solorzano, C. (2017). Characterization of three-dimensional cancer cell migration in mixed collagen-matrigel scaffolds using microfluidics and image analysis. *PLoS One*, *12*(2), e0171417. doi:10.1371/journal.pone.0171417 [doi]
- Ansell, S. M., & Vonderheide, R. H. (2013). Cellular composition of the tumor microenvironment. *American Society of Clinical Oncology Educational Book. American Society of Clinical Oncology Meeting*. doi:10.1200/EdBook_AM.2013.33.e91 [doi]
- Aoyama, Y., & Kitajima, Y. (1999). Pemphigus vulgaris-IgG causes a rapid depletion of desmoglein 3 (Dsg3) from the triton X-100 soluble pools, leading to the formation of Dsg3-depleted desmosomes in a human squamous carcinoma cell line, DJM-1 cells. *The Journal of Investigative Dermatology*, *112*(1), 67-71. doi:10.1046/j.1523-1747.1999.00463.x [doi]
- Astrom, P., Heljasvaara, R., Nyberg, P., Al-Samadi, A., & Salo, T. (2018). Human tumor tissue-based 3D in vitro invasion assays. *Methods in Molecular Biology (Clifton, N.J.)*, *1731*, 213-221. doi:10.1007/978-1-4939-7595-2_19 [doi]
- Astrom, P., Juurikka, K., Hadler-Olsen, E. S., Svineng, G., Cervigne, N. K., Coletta, R. D., . . . Salo, T. (2017). The interplay of matrix metalloproteinase-8, transforming growth factor-beta1 and vascular endothelial growth factor-C cooperatively contributes to the aggressiveness of oral tongue squamous cell carcinoma. *British Journal of Cancer*, *117*(7), 1007-1016. doi:10.1038/bjc.2017.249 [doi]
- Bagan, J., Sarrion, G., & Jimenez, Y. (2010). Oral cancer: Clinical features. *Oral Oncology*, *46*(6), 414-417. doi:10.1016/j.oraloncology.2010.03.009 [doi]
- Balda, M. S., & Matter, K. (2016). Tight junctions as regulators of tissue remodelling. *Current Opinion in Cell Biology*, *42*, 94-101. doi:S0955-0674(16)30092-8 [pii]

- Balkwill, F. R., Capasso, M., & Hagemann, T. (2012). The tumor microenvironment at a glance. *Journal of Cell Science*, *125*(Pt 23), 5591-5596. doi:10.1242/jcs.116392 [doi]
- Baron, S., Hoang, A., Vogel, H., & Attardi, L. D. (2012). Unimpaired skin carcinogenesis in desmoglein 3 knockout mice. *PLoS One*, *7*(11), e50024. doi:10.1371/journal.pone.0050024 [doi]
- Benton, G., Kleinman, H. K., George, J., & Arnaoutova, I. (2011). Multiple uses of basement membrane-like matrix (BME/matrigel) in vitro and in vivo with cancer cells. *International Journal of Cancer*, *128*(8), 1751-1757. doi:10.1002/ijc.25781 [doi]
- Berndt, A., Richter, P., Kosmehl, H., & Franz, M. (2015). Tenascin-C and carcinoma cell invasion in oral and urinary bladder cancer. *Cell Adhesion & Migration*, *9*(1-2), 105-111. doi:10.1080/19336918.2015.1005463 [doi]
- Bitu, C. C., Kauppila, J. H., Bufalino, A., Nurmenniemi, S., Teppo, S., Keinänen, M., . . . Salo, T. (2013). Cathepsin K is present in invasive oral tongue squamous cell carcinoma in vivo and in vitro. *PLoS One*, *8*(8), e70925. doi:10.1371/journal.pone.0070925 [doi]
- Bornslaeger, E. A., Corcoran, C. M., Stappenbeck, T. S., & Green, K. J. (1996). Breaking the connection: Displacement of the desmosomal plaque protein desmoplakin from cell-cell interfaces disrupts anchorage of intermediate filament bundles and alters intercellular junction assembly. *The Journal of Cell Biology*, *134*(4), 985-1001.
- Brooke, M. A., Nitoiu, D., & Kelsell, D. P. (2012). Cell-cell connectivity: Desmosomes and disease. *The Journal of Pathology*, *226*(2), 158-171. doi:10.1002/path.3027 [doi]
- Brown, L., & Wan, H. (2015). Desmoglein 3: A help or a hindrance in cancer progression? *Cancers*, *7*(1), 266-286. doi:10.3390/cancers7010266
- Brown, L., Waseem, A., Cruz, I. N., Szary, J., Gunic, E., Mannan, T., . . . Wan, H. (2014). Desmoglein 3 promotes cancer cell migration and invasion by regulating activator protein 1 and protein kinase C-dependent-ezrin activation. *Oncogene*, *33*(18), 2363-2374. doi:10.1038/onc.2013.186
- Bryne, M., Nielsen, K., Koppang, H. S., & Dabelsteen, E. (1991). Reproducibility of two malignancy grading systems with reportedly prognostic value for oral cancer patients. *Journal of Oral Pathology & Medicine: Official Publication of the International Association of Oral Pathologists and the American Academy of Oral Pathology*, *20*(8), 369-372.
- Cattavarayane, S., Palovuori, R., Tanjore Ramanathan, J., & Manninen, A. (2015). a61- and aV-integrins are required for long-term self-renewal of murine embryonic stem cells in the absence of LIF. *BMC Cell Biology*, *16*(1) doi:10.1186/s12860-015-0051-y
- Chan, E. C., Kuo, S. M., Kong, A. M., Morrison, W. A., Dusting, G. J., Mitchell, G. M., . . . Liu, G. S. (2016). Three dimensional collagen scaffold promotes intrinsic vascularisation for tissue engineering applications. *PLoS One*, *11*(2), e0149799. doi:10.1371/journal.pone.0149799 [doi]
- Chen, Y. J., Chang, J. T., Lee, L., Wang, H. M., Liao, C. T., Chiu, C. C., . . . Cheng, A. J. (2007). DSG3 is overexpressed in head neck cancer and is a potential molecular target for inhibition of oncogenesis. *Oncogene*, *26*(3), 467-476. doi:10.1038/sj.onc.1209802

- Chen, Y. J., Lee, L. Y., Chao, Y. K., Chang, J. T., Lu, Y. C., Li, H. F., . . . Cheng, A. J. (2013). DSG3 facilitates cancer cell growth and invasion through the DSG3-plakoglobin-TCF/LEF-myc/cyclin D1/MMP signaling pathway. *PLoS ONE*, *8*(5), doi:10.1371/journal.pone.0064088
- Culkins, C. C., & Setzer, S. V. (2007). Spotting desmosomes: The first 100 years. *The Journal of Investigative Dermatology*, *127*(E1), 2. doi:10.1038/sj.skinbio.6250010 [doi]
- Dal Maso, L., Torelli, N., Biancotto, E., Di Maso, M., Gini, A., Franchin, G., . . . Polesel, J. (2016). Combined effect of tobacco smoking and alcohol drinking in the risk of head and neck cancers: A re-analysis of case-control studies using bi-dimensional spline models. *European Journal of Epidemiology*, *31*(4), 385-393. doi:10.1007/s10654-015-0028-3 [doi]
- Davisson, M. T., Cook, S. A., Johnson, K. R., & Eicher, E. M. (1994). Balding: A new mutation on mouse chromosome 18 causing hair loss and immunological defects. *The Journal of Heredity*, *85*(2), 134-136.
- Dayan, D., Salo, T., Salo, S., Nyberg, P., Nurmenniemi, S., Costea, D. E., & Vered, M. (2012). Molecular crosstalk between cancer cells and tumor microenvironment components suggests potential targets for new therapeutic approaches in mobile tongue cancer. *Cancer Medicine*, *1*(2), 128-140. doi:10.1002/cam4.24 [doi]
- Del Duca, D., Werbowetski, T., & Del Maestro, R. F. (2004). Spheroid preparation from hanging drops: Characterization of a model of brain tumor invasion. *Journal of Neuro-Oncology*, *67*(3), 295-303.
- Delva, E., Tucker, D. K., & Kowalczyk, A. P. (2009). The desmosome. *Cold Spring Harbor Perspectives in Biology*, *1*(2), a002543. doi:10.1101/cshperspect.a002543 [doi]
- Di Zenzo, G., Di Lullo, G., Corti, D., Calabresi, V., Sinistro, A., Vanzetta, F., . . . Lanzavecchia, A. (2012). Pemphigus autoantibodies generated through somatic mutations target the desmoglein-3 cis-interface. *The Journal of Clinical Investigation*, *122*(10), 3781-3790. doi:10.1172/JCI64413 [doi]
- Dubash, A. D., & Green, K. J. (2011). Desmosomes. *Current Biology: CB*, *21*(14), 529. doi:10.1016/j.cub.2011.04.035 [doi]
- Dusek, R. L., Godsel, L. M., Chen, F., Strohecker, A. M., Getsios, S., Harmon, R., . . . Green, K. J. (2007). Plakoglobin deficiency protects keratinocytes from apoptosis. *The Journal of Investigative Dermatology*, *127*(4), 792-801. doi:S0022-202X(15)33343-1 [pii]
- Edge, S. B., & American Joint Committee on Cancer. (2017). *AJCC cancer staging manual* (Eighth ed.). New York: Springer.
- Engbring, J. A., & Kleinman, H. K. (2003). The basement membrane matrix in malignancy. *The Journal of Pathology*, *200*(4), 465-470. doi:10.1002/path.1396 [doi]
- Fang, Y., & Eglén, R. M. (2017). Three-dimensional cell cultures in drug discovery and development. *SLAS Discovery: Advancing Life Sciences R & D*, *22*(5), 456-472. doi:10.1177/1087057117696795 [doi]
- Ferlay, J., Soerjomataram, I., Dikshit, R., Eser, S., Mathers, C., Rebelo, M., . . . Bray, F. (2015). Cancer incidence and mortality worldwide: Sources, methods and major patterns in GLOBOCAN 2012. *International Journal of Cancer*, *136*(5), 359. doi:10.1002/ijc.29210 [doi]

- Ferlay, J., Soerjomataram, I., Ervik, M., Dikshit, R., Eser, S., Mathers, C., . . . Bray, F. (2013). GLOBOCAN 2012 v1.0, cancer incidence and mortality worldwide: IARC CancerBase no. 11. Retrieved from http://globocan.iarc.fr/Pages/fact_sheets_population.aspx
- Foty, R. (2011). A simple hanging drop cell culture protocol for generation of 3D spheroids. *Journal of Visualized Experiments: JoVE*, (51). pii: 2720. doi:10.3791/2720. doi:10.3791/2720 [doi]
- Frank, J., Cserhalmi-Friedman, P. B., Ahmad, W., Panteleyev, A. A., Aita, V. M., & Christiano, A. M. (2001). Characterization of the desmosomal cadherin gene family: Genomic organization of two desmoglein genes on human chromosome 18q12. *Experimental Dermatology*, 10(2), 90-94. doi:exd100203 [pii]
- Friedl, P., & Brocker, E. B. (2000). The biology of cell locomotion within three-dimensional extracellular matrix. *Cellular and Molecular Life Sciences: CMLS*, 57(1), 41-64. doi:10.1007/s000180050498 [pii]
- Fukuoka, J., Dracheva, T., Shih, J. H., Hewitt, S. M., Fujii, T., Kishor, A., . . . Jen, J. (2007). Desmoglein 3 as a prognostic factor in lung cancer. *Human Pathology*, 38(2), 276-283. doi:S0046-8177(06)00492-8 [pii]
- Garrod, D. (2010). Desmosomes in vivo. *Dermatology Research and Practice*, 2010, 212439. doi:10.1155/2010/212439 [doi]
- Garrod, D. R., Merritt, A. J., & Nie, Z. (2002). Desmosomal cadherins. *Current Opinion in Cell Biology*, 14(5), 537-545. doi:S0955067402003666 [pii]
- Garrod, D., & Chidgey, M. (2008). Desmosome structure, composition and function. *Biochimica Et Biophysica Acta*, 1778(3), 572-587. doi:S0005-2736(07)00275-1 [pii]
- Getsios, S., Simpson, C. L., Kojima, S., Harmon, R., Sheu, L. J., Dusek, R. L., . . . Green, K. J. (2009). Desmoglein 1-dependent suppression of EGFR signaling promotes epidermal differentiation and morphogenesis. *The Journal of Cell Biology*, 185(7), 1243-1258. doi:10.1083/jcb.200809044 [doi]
- Gkretsi, V., Stylianou, A., Papageorgis, P., Polydorou, C., & Stylianopoulos, T. (2015). Remodeling components of the tumor microenvironment to enhance cancer therapy. *Frontiers in Oncology*, 5, 214. doi:10.3389/fonc.2015.00214 [doi]
- Green, K. J., & Jones, J. C. (1996). Desmosomes and hemidesmosomes: Structure and function of molecular components. *FASEB Journal: Official Publication of the Federation of American Societies for Experimental Biology*, 10(8), 871-881.
- Gupta, P. C., & Ray, C. S. (2004). Epidemiology of betel quid usage. *Annals of the Academy of Medicine, Singapore*, 33(4 Suppl), 31-36.
- Hanahan, D., & Weinberg, R. A. (2011). Hallmarks of cancer: The next generation. *Cell*, 144(5), 646-674. doi:10.1016/j.cell.2011.02.013 [doi]
- Harjanto, D., & Zaman, M. H. (2013). Modeling extracellular matrix reorganization in 3D environments. *PloS One*, 8(1), e52509. doi:10.1371/journal.pone.0052509 [doi]
- Harma, V., Schukov, H. P., Happonen, A., Ahonen, I., Virtanen, J., Siitari, H., . . . Nees, M. (2014). Quantification of dynamic morphological drug responses in 3D organotypic cell cultures by automated image analysis. *PloS One*, 9(5), e96426. doi:10.1371/journal.pone.0096426 [doi]

- Hartlieb, E., Kempf, B., Partilla, M., Vigh, B., Spindler, V., & Waschke, J. (2013). Desmoglein 2 is less important than desmoglein 3 for keratinocyte cohesion. *PLoS One*, 8(1), e53739. doi:10.1371/journal.pone.0053739 [doi]
- Homann, N., Tillonen, J., Rintamaki, H., Salaspuro, M., Lindqvist, C., & Meurman, J. H. (2001). Poor dental status increases acetaldehyde production from ethanol in saliva: A possible link to increased oral cancer risk among heavy drinkers. *Oral Oncology*, 37(2), 153-158. doi:S1368837500000762 [pii]
- Hughes, C. S., Postovit, L. M., & Lajoie, G. A. (2010). Matrigel: A complex protein mixture required for optimal growth of cell culture. *Proteomics*, 10(9), 1886-1890. doi:10.1002/pmic.200900758 [doi]
- Jadhav, K. B., & Gupta, N. (2013). Clinicopathological prognostic implicators of oral squamous cell carcinoma: Need to understand and revise. *North American Journal of Medical Sciences*, 5(12), 671-679. doi:10.4103/1947-2714.123239 [doi]
- Jaganathan, H., Gage, J., Leonard, F., Srinivasan, S., Souza, G. R., Dave, B., & Godin, B. (2014). Three-dimensional in vitro co-culture model of breast tumor using magnetic levitation. *Scientific Reports*, 4 doi:10.1038/srep06468
- Janmey, P. A., Winer, J. P., & Weisel, J. W. (2009). Fibrin gels and their clinical and bioengineering applications. *Journal of the Royal Society, Interface*, 6(30), 1-10. doi:10.1098/rsif.2008.0327 [doi]
- Jennings, J. M., Tucker, D. K., Kottke, M. D., Saito, M., Delva, E., Hanakawa, Y., . . . Kowalczyk, A. P. (2011). Desmosome disassembly in response to pemphigus vulgaris IgG occurs in distinct phases and can be reversed by expression of exogenous Dsg3. *The Journal of Investigative Dermatology*, 131(3), 706-718. doi:10.1038/jid.2010.389 [doi]
- Johnson, J. L., Koetsier, J. L., Sirico, A., Agidi, A. T., Antonini, D., Missero, C., & Green, K. J. (2014). The desmosomal protein desmoglein 1 aids recovery of epidermal differentiation after acute UV light exposure. *The Journal of Investigative Dermatology*, 134(8), 2154-2162. doi:S0022-202X(15)36951-7 [pii]
- Jones, K. B., & Klein, O. D. (2013). Oral epithelial stem cells in tissue maintenance and disease: The first steps in a long journey. *International Journal of Oral Science*, 5(3), 121-129. doi:10.1038/ijos.2013.46 [doi]
- Joshi, P., Dutta, S., Chaturvedi, P., & Nair, S. (2014). Head and neck cancers in developing countries. *Rambam Maimonides Medical Journal*, 5(2), e0009. doi:10.5041/RMMJ.10143 [doi]
- Joyce, J. A., & Pollard, J. W. (2009). Microenvironmental regulation of metastasis. *Nature Reviews.Cancer*, 9(4), 239-252. doi:10.1038/nrc2618 [doi]
- Justus, C. R., Leffler, N., Ruiz-Echevarria, M., & Yang, L. V. (2014). In vitro cell migration and invasion assays. *Journal of Visualized Experiments: JoVE*, (88). doi(88), 10.3791/51046. doi:10.3791/51046 [doi]
- Katt, M. E., Placone, A. L., Wong, A. D., Xu, Z. S., & Searson, P. C. (2016). In vitro tumor models: Advantages, disadvantages, variables, and selecting the right platform. *Frontiers in Bioengineering and Biotechnology*, 4, 12. doi:10.3389/fbioe.2016.00012 [doi]

- Kim, I. H., & Myoung, H. (2017). Squamous cell carcinoma of the buccal mucosa involving the masticator space: A case report. *Journal of the Korean Association of Oral and Maxillofacial Surgeons*, 43(3), 191-196. doi:10.5125/jkaoms.2017.43.3.191 [doi]
- Kim, J., Kim, S., Park, H., Lee, S., Lee, S., & Kim, S. (2018). 739 suprabasal acantholytic blisters in oral mucosa caused by homozygous nonsense mutation in desmoglein 3 gene [Abstract]. *Journal of Investigative Dermatology*, 138(5, Supplement) S126. doi:10.1016/j.jid.2018.03.749 Retrieved from <http://www.sciencedirect.com/science/article/pii/S0022202X18309758>
- Kitajima, Y. (2002). Mechanisms of desmosome assembly and disassembly. *Clinical and Experimental Dermatology*, 27(8), 684-690. doi:1116 [pii]
- Kleinman, H. K., & Martin, G. R. (2005). Matrigel: Basement membrane matrix with biological activity. *Seminars in Cancer Biology*, 15(5), 378-386. doi:S1044-579X(05)00031-3 [pii]
- Kleinman, H. K., McGarvey, M. L., Hassell, J. R., Star, V. L., Cannon, F. B., Laurie, G. W., & Martin, G. R. (1986). Basement membrane complexes with biological activity. *Biochemistry*, 25(2), 312-318.
- Koch, P. J., Mahoney, M. G., Ishikawa, H., Pulkkinen, L., Uitto, J., Shultz, L., . . . Stanley, J. R. (1997). Targeted disruption of the pemphigus vulgaris antigen (desmoglein 3) gene in mice causes loss of keratinocyte cell adhesion with a phenotype similar to pemphigus vulgaris. *The Journal of Cell Biology*, 137(5), 1091-1102.
- Kolegraff, K., Nava, P., Helms, M. N., Parkos, C. A., & Nusrat, A. (2011). Loss of desmocollin-2 confers a tumorigenic phenotype to colonic epithelial cells through activation of akt/beta-catenin signaling. *Molecular Biology of the Cell*, 22(8), 1121-1134. doi:10.1091/mbc.E10-10-0845 [doi]
- Korvala, J., Harjula, T., Siirila, K., Almangush, A., Aro, K., Makitie, A. A., . . . Salo, T. (2014). Toll-like receptor 9 expression in mucoepidermoid salivary gland carcinoma may associate with good prognosis. *Journal of Oral Pathology & Medicine: Official Publication of the International Association of Oral Pathologists and the American Academy of Oral Pathology*, 43(7), 530-537. doi:10.1111/jop.12160 [doi]
- Kouno, M., Minabe, M., Tachikawa, T., & Stanley, J. R. (2017). Oral cancer treatment by targeted drug delivery system with an anti-desmoglein monoclonal antibody [Abstract]. *Journal of Dermatological Science*, 86(2) e27. doi:10.1016/j.jdermsci.2017.02.078
- Kramer, N., Walzl, A., Unger, C., Rosner, M., Krupitza, G., Hengstschlager, M., & Dolznig, H. (2013). In vitro cell migration and invasion assays. *Mutation Research*, 752(1), 10-24. doi:10.1016/j.mrrev.2012.08.001 [doi]
- Kulasekara, K. K., Lukandu, O. M., Neppelberg, E., Vintermyr, O. K., Johannessen, A. C., & Costea, D. E. (2009). Cancer progression is associated with increased expression of basement membrane proteins in three-dimensional in vitro models of human oral cancer. *Archives of Oral Biology*, 54(10), 924-931. doi:10.1016/j.archoralbio.2009.07.004 [doi]

- Laaksonen, M., Suojanen, J., Nurmenniemi, S., Lr, E., Sorsa, T., & Salo, T. (2008). The enamel matrix derivative (emdogain) enhances human tongue carcinoma cells gelatinase production, migration and metastasis formation. *Oral Oncology*, *44*(8), 733-742. doi:10.1016/j.oraloncology.2007.09.008
- LeBleu, V. S., Macdonald, B., & Kalluri, R. (2007). Structure and function of basement membranes. *Experimental Biology and Medicine (Maywood, N.J.)*, *232*(9), 1121-1129. doi:232/9/1121 [pii]
- Lee, J. S., Yoon, H. K., Sohn, K. C., Back, S. J., Kee, S. H., Seo, Y. J., . . . Lee, J. H. (2009). Expression of N-terminal truncated desmoglein 3 (deltaNDg3) in epidermis and its role in keratinocyte differentiation. *Experimental & Molecular Medicine*, *41*(1), 42-50. doi:20091316 [pii]
- Lin, R. Z., & Chang, H. Y. (2008). Recent advances in three-dimensional multicellular spheroid culture for biomedical research. *Biotechnology Journal*, *3*(9-10), 1172-1184. doi:10.1002/biot.200700228 [doi]
- Listl, S., Jansen, L., Stenzinger, A., Freier, K., Emrich, K., Holleczeck, B., . . . GEKID Cancer Survival Working Group. (2013). Survival of patients with oral cavity cancer in germany. *PLoS One*, *8*(1), e53415. doi:10.1371/journal.pone.0053415 [doi]
- Lydiatt, W. M., Patel, S. G., O'Sullivan, B., Brandwein, M. S., Ridge, J. A., Migliacci, J. C., . . . Shah, J. P. (2017). Head and neck cancers-major changes in the american joint committee on cancer eighth edition cancer staging manual. *CA: A Cancer Journal for Clinicians*, *67*(2), 122-137. doi:10.3322/caac.21389 [doi]
- Mannan, T., Jing, S., Foroushania, S. H., Fortune, F., & Wan, H. (2011). RNAi-mediated inhibition of the desmosomal cadherin (desmoglein 3) impairs epithelial cell proliferation. *Cell Proliferation*, *44*(4), 301-310. doi:10.1111/j.1365-2184.2011.00765.x [doi]
- Marshall, J. (2011). Transwell((R)) invasion assays. *Methods in Molecular Biology (Clifton, N.J.)*, *769*, 97-110. doi:10.1007/978-1-61779-207-6_8 [doi]
- Mehta, G., Hsiao, A. Y., Ingram, M., Luker, G. D., & Takayama, S. (2012). Opportunities and challenges for use of tumor spheroids as models to test drug delivery and efficacy. *Journal of Controlled Release: Official Journal of the Controlled Release Society*, *164*(2), 192-204. doi:10.1016/j.jconrel.2012.04.045 [doi]
- Merikallio, H., Turpeenniemi-Hujanen, T., Paakko, P., Makitaro, R., Riitta, K., Salo, S., . . . Soini, Y. (2012). Snail promotes an invasive phenotype in lung carcinoma. *Respiratory Research*, *13*, 104. doi:10.1186/1465-9921-13-104 [doi]
- Merritt, A. J., Berika, M. Y., Zhai, W., Kirk, S. E., Ji, B., Hardman, M. J., & Garrod, D. R. (2002). Suprabasal desmoglein 3 expression in the epidermis of transgenic mice results in hyperproliferation and abnormal differentiation. *Molecular and Cellular Biology*, *22*(16), 5846-5858.
- Mese, G., Richard, G., & White, T. W. (2007). Gap junctions: Basic structure and function. *The Journal of Investigative Dermatology*, *127*(11), 2516-2524. doi:S0022-202X(15)33182-1 [pii]

- Mocellin, S., Wang, E., & Marincola, F. M. (2001). Cytokines and immune response in the tumor microenvironment. *Journal of Immunotherapy (Hagerstown, Md.: 1997)*, 24(5), 392-407.
- Moftah, H., Dias, K., Apu, E. H., Liu, L., Uttagomol, J., Bergmeier, L., . . . Wan, H. (2016). Desmoglein 3 regulates membrane trafficking of cadherins, an implication in cell-cell adhesion. *Cell Adhesion & Migration*, , 1-22. doi:10.1080/19336918.2016.1195942 [doi]
- Montagutelli, X., Lalouette, A., Boulouis, H. J., Guenet, J. L., & Sundberg, J. P. (1997). Vesicle formation and follicular root sheath separation in mice homozygous for deleterious alleles at the balding (bal) locus. *The Journal of Investigative Dermatology*, 109(3), 324-328. doi:S0022-202X(15)42994-X [pii]
- Morin, K. T., & Tranquillo, R. T. (2013). In vitro models of angiogenesis and vasculogenesis in fibrin gel. *Experimental Cell Research*, 319(16), 2409-2417. doi:10.1016/j.yexcr.2013.06.006 [doi]
- Mroueh, R., Haapaniemi, A., Grenman, R., Laranne, J., Pukkila, M., Almangush, A., . . . Makitie, A. (2017). Improved outcomes with oral tongue squamous cell carcinoma in Finland. *Head & Neck*, 39(7), 1306-1312. doi:10.1002/hed.24744 [doi]
- Mruk, D. D., Silvestrini, B., & Cheng, C. Y. (2008). Anchoring junctions as drug targets: Role in contraceptive development. *Pharmacological Reviews*, 60(2), 146-180. doi:10.1124/pr.107.07105 [doi]
- Nagafuchi, A. (2001). Molecular architecture of adherens junctions. *Current Opinion in Cell Biology*, 13(5), 600-603. doi:S0955-0674(00)00257-X [pii]
- Niessen, C. M., & Gottardi, C. J. (2008). Molecular components of the adherens junction. *Biochimica Et Biophysica Acta*, 1778(3), 562-571. doi:10.1016/j.bbamem.2007.12.015 [doi]
- North, A. J., Bardsley, W. G., Hyam, J., Bornslaeger, E. A., Cordingley, H. C., Trinnaman, B., . . . Garrod, D. R. (1999). Molecular map of the desmosomal plaque. *Journal of Cell Science*, 112 (Pt 23)(Pt 23), 4325-4336.
- Nurmenniemi, S., Kuvaja, P., Lehtonen, S., Tiuraniemi, S., Alahuhta, I., Mattila, R. K., . . . Lehenkari, P. (2010). Toll-like receptor 9 ligands enhance mesenchymal stem cell invasion and expression of matrix metalloprotease-13. *Experimental Cell Research*, 316(16), 2676-2682. doi:10.1016/j.yexcr.2010.05.024 [doi]
- Nurmenniemi, S., Sinikumpu, T., Alahuhta, I., Salo, S., Sutinen, M., Santala, M., . . . Salo, T. (2009). A novel organotypic model mimics the tumor microenvironment. *American Journal of Pathology*, 175(3), 1281-1291. doi:10.2353/ajpath.2009.081110
- Patel, V., Martin, D., Malhotra, R., Marsh, C. A., Doci, C. L., Veenstra, T. D., . . . Gutkind, J. S. (2013). DSG3 as a biomarker for the ultrasensitive detection of occult lymph node metastasis in oral cancer using nanostructured immunoarrays. *Oral Oncology*, 49(2), 93-101. doi:10.1016/j.oraloncology.2012.08.001 [doi]
- Paulsson, M. (1992). Basement membrane proteins: Structure, assembly, and cellular interactions. *Critical Reviews in Biochemistry and Molecular Biology*, 27(1-2), 93-127. doi:10.3109/10409239209082560 [doi]

- Payne, A. S., Hanakawa, Y., Amagai, M., & Stanley, J. R. (2004). Desmosomes and disease: Pemphigus and bullous impetigo. *Current Opinion in Cell Biology*, *16*(5), 536-543. doi:10.1016/j.ceb.2004.07.006 [doi]
- Pirila, E., Vayrynen, O., Sundquist, E., Pakkila, K., Nyberg, P., Nurmenniemi, S., . . . Salo, T. (2015). Macrophages modulate migration and invasion of human tongue squamous cell carcinoma. *PLoS One*, *10*(3), e0120895. doi:10.1371/journal.pone.0120895 [doi]
- Porter, S. R., Lodi, G., Chandler, K., & Kumar, N. (1997). Development of squamous cell carcinoma in hepatitis C virus-associated lichen planus. *Oral Oncology*, *33*(1), 58-59.
- Puente, X. S., Sanchez, L. M., Overall, C. M., & Lopez-Otin, C. (2003). Human and mouse proteases: A comparative genomic approach. *Nature Reviews Genetics*, *4*(7), 544-558. doi:10.1038/nrg1111 [doi]
- Pulkkinen, L., Choi, Y. W., Simpson, A., Montagutelli, X., Sundberg, J., Uitto, J., & Mahoney, M. G. (2002). Loss of cell adhesion in Dsg3bal-pas mice with homozygous deletion mutation (2079del14) in the desmoglein 3 gene. *The Journal of Investigative Dermatology*, *119*(6), 1237-1243. doi:S0022-202X(15)30081-6 [pii]
- Quail, D. F., & Joyce, J. A. (2013). Microenvironmental regulation of tumor progression and metastasis. *Nature Medicine*, *19*(11), 1423-1437. doi:10.1038/nm.3394 [doi]
- Rangarajan, R., & Zaman, M. H. (2008). Modeling cell migration in 3D: Status and challenges. *Cell Adhesion & Migration*, *2*(2), 106-109. doi:6211 [pii]
- Ricard-Blum, S. (2011). The collagen family. *Cold Spring Harbor Perspectives in Biology*, *3*(1), a004978. doi:10.1101/cshperspect.a004978 [doi]
- Rodriguez, T., Altieri, A., Chatenoud, L., Gallus, S., Bosetti, C., Negri, E., . . . La Vecchia, C. (2004). Risk factors for oral and pharyngeal cancer in young adults. *Oral Oncology*, *40*(2), 207-213. doi:S1368837503001684 [pii]
- Rotzer, V., Hartlieb, E., Vielmuth, F., Gliem, M., Spindler, V., & Waschke, J. (2015). E-cadherin and src associate with extradesmosomal Dsg3 and modulate desmosome assembly and adhesion. *Cellular and Molecular Life Sciences: CMLS*, *72*(24), 4885-4897. doi:10.1007/s00018-015-1977-0 [doi]
- Rotzer, V., Hartlieb, E., Winkler, J., Walter, E., Schlipp, A., Sardy, M., . . . Waschke, J. (2015). Desmoglein 3-dependent signaling regulates keratinocyte migration and wound healing. *The Journal of Investigative Dermatology*, doi:10.1038/jid.2015.380 [doi]
- Ruocco, V., Ruocco, E., Lo Schiavo, A., Brunetti, G., Guerrero, L. P., & Wolf, R. (2013). Pemphigus: Etiology, pathogenesis, and inducing or triggering factors: Facts and controversies. *Clinics in Dermatology*, *31*(4), 374-381. doi:S0738-081X(13)00005-9 [pii]
- Saito, M., Tucker, D. K., Kohlhorst, D., Niessen, C. M., & Kowalczyk, A. P. (2012). Classical and desmosomal cadherins at a glance. *Journal of Cell Science*, *125*(Pt 11), 2547-2552. doi:10.1242/jcs.066654 [doi]
- Salo, S., Bitu, C., Merkkü, K., Nyberg, P., Bello, I. O., Vuoristo, J., . . . Salo, T. (2013). Human bone marrow mesenchymal stem cells induce collagen production and tongue cancer invasion. *PLoS One*, *8*(10), e77692. doi:10.1371/journal.pone.0077692 [doi]

- Salo, T., Dourado, M. R., Sundquist, E., Apu, E. H., Alahuhta, I., Tuomainen, K., . . . Al-Samadi, A. (2018). Organotypic three-dimensional assays based on human leiomyoma-derived matrices. *Philosophical Transactions of the Royal Society of London. Series B, Biological Sciences*, 373(1737), 10.1098/rstb.2016.0482. doi:20160482 [pii]
- Salo, T., Sutinen, M., Hoque Apu, E., Sundquist, E., Cervigne, N. K., de Oliveira, C. E., . . . Coletta, R. D. (2015). A novel human leiomyoma tissue derived matrix for cell culture studies. *BMC Cancer*, 15(1), 1. doi:10.1186/s12885-015-1944-z
- Salo, T., Vered, M., Bello, I. O., Nyberg, P., Bitu, C. C., Zlotogorski Hurvitz, A., & Dayan, D. (2014). Insights into the role of components of the tumor microenvironment in oral carcinoma call for new therapeutic approaches. *Experimental Cell Research*, 325(2), 58-64. doi:10.1016/j.yexcr.2013.12.029 [doi]
- Sano, D., & Myers, J. N. (2007). Metastasis of squamous cell carcinoma of the oral tongue. *Cancer Metastasis Reviews*, 26(3-4), 645-662. doi:10.1007/s10555-007-9082-y [doi]
- Sathiyasekar, A. C., Chandrasekar, P., Pakash, A., Kumar, K. U., & Jaishlal, M. S. (2016). Overview of immunology of oral squamous cell carcinoma. *Journal of Pharmacy & Bioallied Sciences*, 8(Suppl 1), S12. doi:10.4103/0975-7406.191974 [doi]
- Schense, J. C., & Hubbell, J. A. (1999). Cross-linking exogenous bifunctional peptides into fibrin gels with factor XIIIa. *Bioconjugate Chemistry*, 10(1), 75-81. doi:10.1021/bc9800769 [doi]
- Schmidt, A., & Koch, P. J. (2007). Desmosomes: Just cell adhesion or is there more? *Cell Adhesion & Migration*, 1(1), 28-32. doi:4204 [pii]
- Scully, C., & Bagan, J. (2009). Oral squamous cell carcinoma overview. *Oral Oncology*, 45(4-5), 301-308. doi:10.1016/j.oraloncology.2009.01.004 [doi]
- Shah, J. P., & Gil, Z. (2009). Current concepts in management of oral cancer--surgery. *Oral Oncology*, 45(4-5), 394-401. doi:10.1016/j.oraloncology.2008.05.017 [doi]
- Shaikh, M. H., Khan, A. I., Sadat, A., Chowdhury, A. H., Jinnah, S. A., Gopalan, V., . . . Johnson, N. W. (2017). Prevalence and types of high-risk human papillomaviruses in head and neck cancers from Bangladesh. *BMC Cancer*, 17(1), 0. doi:10.1186/s12885-017-3789-0 [doi]
- Shamir, E. R., & Ewald, A. J. (2014). Three-dimensional organotypic culture: Experimental models of mammalian biology and disease. *Nature Reviews. Molecular Cell Biology*, 15(10), 647-664. doi:10.1038/nrm3873 [doi]
- Shetty, S., & Gokul, S. (2012). Keratinization and its disorders. *Oman Medical Journal*, 27(5), 348-357. doi:10.5001/omj.2012.90 [doi]
- Shield, K. D., Ferlay, J., Jemal, A., Sankaranarayanan, R., Chaturvedi, A. K., Bray, F., & Soerjomataram, I. (2017). The global incidence of lip, oral cavity, and pharyngeal cancers by subsite in 2012. *CA: A Cancer Journal for Clinicians*, 67(1), 51-64. doi:10.3322/caac.21384 [doi]

- Shiose, S., Hata, Y., Noda, Y., Sassa, Y., Takeda, A., Yoshikawa, H., . . . Ishibashi, T. (2004). Fibrinogen stimulates in vitro angiogenesis by choroidal endothelial cells via autocrine VEGF. *Graefes Archive for Clinical and Experimental Ophthalmology = Albrecht Von Graefes Archiv Fur Klinische Und Experimentelle Ophthalmologie*, 242(9), 777-783. doi:10.1007/s00417-004-0910-2 [doi]
- Sobral, L. M., Bufalino, A., Lopes, M. A., Graner, E., Salo, T., & Coletta, R. D. (2011). Myofibroblasts in the stroma of oral cancer promote tumorigenesis via secretion of activin A. *Oral Oncology*, 47(9), 840-846. doi:10.1016/j.oraloncology.2011.06.011
- Sultana, J., Bashar, A., & Molla, M. R. (2014). New management strategies of oral tongue cancer in Bangladesh. *Journal of Maxillofacial and Oral Surgery*, 13(4), 394-400. doi:10.1007/s12663-013-0566-8 [doi]
- Sundquist, E., Kauppila, J. H., Veijola, J., Mroueh, R., Lehenkari, P., Laitinen, S., . . . Salo, T. (2017). Tenascin-C and fibronectin expression divide early stage tongue cancer into low- and high-risk groups. *British Journal of Cancer*, 116(5), 640-648. doi:10.1038/bjc.2016.455 [doi]
- Sundquist, E., Renko, O., Salo, S., Magga, J., Cervigne, N. K., Nyberg, P., . . . Salo, T. (2016). Neoplastic extracellular matrix environment promotes cancer invasion in vitro. *Experimental Cell Research*, 344(2), 229-240. doi:10.1016/j.yexcr.2016.04.003 [doi]
- Taghavi, N., & Yazdi, I. (2007). Type of food and risk of oral cancer. *Archives of Iranian Medicine*, 10(2), 227-232. doi:0017 [pii]
- Tanjore, H., & Kalluri, R. (2006). The role of type IV collagen and basement membranes in cancer progression and metastasis. *The American Journal of Pathology*, 168(3), 715-717. doi:S0002-9440(10)62131-1 [pii]
- Teh, M. T., Parkinson, E. K., Thurlow, J. K., Liu, F., Fortune, F., & Wan, H. (2011). A molecular study of desmosomes identifies a desmoglein isoform switch in head and neck squamous cell carcinoma. *Journal of Oral Pathology & Medicine: Official Publication of the International Association of Oral Pathologists and the American Academy of Oral Pathology*, 40(1), 67-76. doi:10.1111/j.1600-0714.2010.00951.x [doi]
- Teppo, S., Sundquist, E., Vered, M., Holappa, H., Parkkisenniemi, J., Rinaldi, T., . . . Nyberg, P. (2013). The hypoxic tumor microenvironment regulates invasion of aggressive oral carcinoma cells. *Experimental Cell Research*, 319(4), 376-389. doi:10.1016/j.yexcr.2012.12.010 [doi]
- Thomason, H. A., Scothern, A., McHarg, S., & Garrod, D. R. (2010). Desmosomes: Adhesive strength and signalling in health and disease. *The Biochemical Journal*, 429(3), 419-433. doi:10.1042/BJ20100567 [doi]
- Tsang, S. M., Brown, L., Gadmor, H., Gammon, L., Fortune, F., Wheeler, A., & Wan, H. (2012). Desmoglein 3 acting as an upstream regulator of rho GTPases, rac-1/Cdc42 in the regulation of actin organisation and dynamics. *Experimental Cell Research*, 318(18), 2269-2283. doi:10.1016/j.yexcr.2012.07.002 [doi]

- Tsang, S. M., Brown, L., Lin, K., Liu, L., Piper, K., O'Toole, E. A., . . . Wan, H. (2012). Non-junctional human desmoglein 3 acts as an upstream regulator of src in E-cadherin adhesion, a pathway possibly involved in the pathogenesis of pemphigus vulgaris. *The Journal of Pathology*, 227(1), 81-93. doi:10.1002/path.3982 [doi]
- Tsang, S. M., Liu, L., Teh, M. -, Wheeler, A., Grose, R., Hart, I. R., . . . Wan, H. (2010). Desmoglein 3, via an interaction with E-cadherin, is associated with activation of src. *PLoS ONE*, 5(12) doi:10.1371/journal.pone.0014211
- Tsunoda, K., Ota, T., Aoki, M., Yamada, T., Nagai, T., Nakagawa, T., . . . Amagai, M. (2003). Induction of pemphigus phenotype by a mouse monoclonal antibody against the amino-terminal adhesive interface of desmoglein 3. *Journal of Immunology (Baltimore, Md.: 1950)*, 170(4), 2170-2178.
- Van Goethem, E., Poincloux, R., Gauffre, F., Maridonneau-Parini, I., & Le Cabec, V. (2010). Matrix architecture dictates three-dimensional migration modes of human macrophages: Differential involvement of proteases and podosome-like structures. *Journal of Immunology*, 184(2), 1049-1061. doi:10.4049/jimmunol.0902223
- Vered, M., Lehtonen, M., Hotakainen, L., Pirila, E., Teppo, S., Nyberg, P., . . . Dayan, D. (2015). Caveolin-1 accumulation in the tongue cancer tumor microenvironment is significantly associated with poor prognosis: An in-vivo and in-vitro study. *BMC Cancer*, 15, 6. doi:10.1186/s12885-015-1030-6 [doi]
- Vilen, S. T., Suojanen, J., Salas, F., Risteli, J., Ylipalosaari, M., Itkonen, O., . . . Nyberg, P. (2012). Trypsin-2 enhances carcinoma invasion by processing tight junctions and activating ProMT1-MMP. *Cancer Investigation*, 30(8), 583-592. doi:10.3109/07357907.2012.716467 [doi]
- Vinci, M., Gowan, S., Boxall, F., Patterson, L., Zimmermann, M., Court, W., . . . Eccles, S. A. (2012). Advances in establishment and analysis of three-dimensional tumor spheroid-based functional assays for target validation and drug evaluation. *BMC Biology*, 10, 29. doi:10.1186/1741-7007-10-29 [doi]
- Wan, H. (2018). Desmoglein-3. In S. Choi (Ed.), *Encyclopedia of signaling molecules* (pp. 1352-1366). Cham: Springer International Publishing. doi:10.1007/978-3-319-67199-4_101583 Retrieved from https://doi.org/10.1007/978-3-319-67199-4_101583
- Wang, M., Zhao, J., Zhang, L., Wei, F., Lian, Y., Wu, Y., . . . Guo, C. (2017). Role of tumor microenvironment in tumorigenesis. *Journal of Cancer*, 8(5), 761-773. doi:10.7150/jca.17648 [doi]
- Warnakulasuriya, S., Trivedy, C., & Peters, T. J. (2002). Areca nut use: An independent risk factor for oral cancer. *BMJ (Clinical Research Ed.)*, 324(7341), 799-800.
- Wells, R. G. (2008). The role of matrix stiffness in regulating cell behavior. *Hepatology (Baltimore, Md.)*, 47(4), 1394-1400. doi:10.1002/hep.22193 [doi]
- Windoffer, R., Borchert-Stuhltrager, M., & Leube, R. E. (2002). Desmosomes: Interconnected calcium-dependent structures of remarkable stability with significant integral membrane protein turnover. *Journal of Cell Science*, 115(Pt 8), 1717-1732.
- Winning, T. A., & Townsend, G. C. (2000). Oral mucosal embryology and histology. *Clinics in Dermatology*, 18(5), 499-511. doi:S0738-081X(00)00140-1 [pii]

- Wolf, K., & Friedl, P. (2011). Extracellular matrix determinants of proteolytic and non-proteolytic cell migration. *Trends in Cell Biology*, *21*(12), 736-744. doi:10.1016/j.tcb.2011.09.006 [doi]
- Xu, J., Yang, X. X., Wu, Y. G., Li, X. Y., & Bai, B. (2014). Meat consumption and risk of oral cavity and oropharynx cancer: A meta-analysis of observational studies. *PloS One*, *9*(4), e95048. doi:10.1371/journal.pone.0095048 [doi]
- Yamamoto, V. N., Thylur, D. S., Bauschard, M., Schmale, I., & Sinha, U. K. (2016). Overcoming radioresistance in head and neck squamous cell carcinoma. *Oral Oncology*, *63*, 44-51. doi:S1368-8375(16)30208-1 [pii]
- Yannas, I. V., Tzeranis, D. S., Harley, B. A., & So, P. T. (2010). Biologically active collagen-based scaffolds: Advances in processing and characterization. *Philosophical Transactions. Series A, Mathematical, Physical, and Engineering Sciences*, *368*(1917), 2123-2139. doi:10.1098/rsta.2010.0015 [doi]
- Yee, N. S., Ignatenko, N., Finnberg, N., Lee, N., & Stairs, D. (2015). Animal models of cancer biology. *Cancer Growth and Metastasis*, *8*(Suppl 1), 115-118. doi:10.4137/CGM.S37907 [doi]
- Yin, T., & Green, K. J. (2004). Regulation of desmosome assembly and adhesion. *Seminars in Cell & Developmental Biology*, *15*(6), 665-677. doi:S1084-9521(04)00091-6 [pii]
- Yokouchi, M., & Kubo, A. (2018). Maintenance of tight junction barrier integrity in cell turnover and skin diseases. *Experimental Dermatology*, doi:10.1111/exd.13742 [doi]
- Zaman, M. H., Trapani, L. M., Sieminski, A. L., Mackellar, D., Gong, H., Kamm, R. D., . . . Matsudaira, P. (2006). Migration of tumor cells in 3D matrices is governed by matrix stiffness along with cell-matrix adhesion and proteolysis. *Proceedings of the National Academy of Sciences of the United States of America*, *103*(29), 10889-10894. doi:0604460103 [pii]
- Zhang, X., Nie, D., & Chakrabarty, S. (2010). Growth factors in tumor microenvironment. *Frontiers in Bioscience (Landmark Edition)*, *15*, 151-165. doi:3612 [pii]
- Zhao, H., Ma, L., Zhou, J., Mao, Z., Gao, C., & Shen, J. (2008). Fabrication and physical and biological properties of fibrin gel derived from human plasma. *Biomedical Materials (Bristol, England)*, *3*(1), 6041/3/1/015001. Epub 2007 Dec 19. doi:10.1088/1748-6041/3/1/015001 [doi]

Original publications

- I Moftah H, Dias K, Hoque Apu E, Liu L, Uttagamol J, Bergmeier L, Kermorgant S & Wan H. (2017). Desmoglein 3 regulates membrane trafficking of cadherins, an implication in cell-cell adhesion. *Cell Adh Migr*, 11 (3), 211-232.
- II Salo T, Sutinen M, Hoque Apu E, Sundquist E, Cervigne N, Oliveira CE, Akram SU, Ohlmeier S, Suomi F, Eklund L, Juusela P, Åström P, Bitu CC, Santala M, Savolainen K, Korvala J, Paes Leme AF & Coletta RD. (2015). A novel human leiomyoma tissue derived matrix for cell culture studies. *BMC Cancer*, 15:981.
- III Hoque Apu E, Akram SU, Rissanen J, Wan H & Salo T. (2018). Desmoglein 3 – influence on oral carcinoma cell migration and invasion. *Exp Cell Res*, 370 (2), 376-389.

Reprinted with permission from Taylor & Francis (I), Springer Nature (II) and Elsevier Limited (III).

Original publications are not included in the electronic version of the dissertation.

1466. Matinolli, Hanna-Maria (2018) Nutrition and early life programming of health : focus on preterm birth and infant feeding in relation to energy-balance and related traits in adulthood
1467. Tikanmäki, Marjaana (2018) Preterm birth and parental and pregnancy related factors in association with physical activity and fitness in adolescence and young adulthood
1468. Juvonen-Posti, Pirjo (2018) Work-related rehabilitation for strengthening working careers : a multiperspective and mixed methods study of its mechanisms
1469. Palaniswamy, Saranya (2018) Vitamin D status and its association with leukocyte telomere length, obesity and inflammation in young adults : a Northern Finland Birth Cohort 1966 study
1470. Bur, Hamid (2018) Biological prognostic and predictive markers in Hodgkin lymphoma
1471. Haapanen, Henri (2018) Preconditioning against ischemic injury of the central nervous system in aortic surgery : an experimental study in a porcine model with remote ischemic preconditioning and diazoxide
1472. Mahlman, Mari (2018) Genetic background and antenatal risk factors of bronchopulmonary dysplasia
1473. Lantto, Ulla (2018) Etiology and outcome of PFAPA (periodic fever, aphthous stomatitis, pharyngitis and adenitis) syndrome among patients operated with tonsillectomy in childhood
1474. Hintsala, Heidi (2018) Cardiovascular responses to cold exposure in untreated hypertension
1475. Alakortes, Jaana (2018) Social-emotional and behavioral development problems in 1 to 2-year-old children in Northern Finland : reports of mothers, fathers and healthcare professionals
1476. Puhto, Teija (2018) The burden of healthcare-associated infections in primary and tertiary healthcare wards and the cost of procedure-related prosthetic joint infections
1477. Honkila, Minna (2018) *Chlamydia trachomatis* infections in neonates and infants
1478. Krooks, Laura (2018) Malocclusions in relation to facial soft tissue characteristics, facial aesthetics and temporomandibular disorders in the Northern Finland Birth Cohort 1966

S E R I E S E D I T O R S

A
SCIENTIAE RERUM NATURALIUM
University Lecturer Tuomo Glumoff

B
HUMANIORA
University Lecturer Santeri Palviainen

C
TECHNICA
Postdoctoral research fellow Sanna Taskila

D
MEDICA
Professor Olli Vuolteenaho

E
SCIENTIAE RERUM SOCIALIUM
University Lecturer Veli-Matti Ulvinen

E
SCRIPTA ACADEMICA
Planning Director Pertti Tikkanen

G
OECONOMICA
Professor Jari Juga

H
ARCHITECTONICA
University Lecturer Anu Soikkeli

EDITOR IN CHIEF
Professor Olli Vuolteenaho

PUBLICATIONS EDITOR
Publications Editor Kirsti Nurkkala

